Title
Immunohistochemical expression analysis of the human fetal lower urogenital tract

Authors
Shen, Joel
Isaacson, Dylan
Cao, Mei
et al.

Publication Date
2018-09-01

DOI
10.1016/j.diff.2018.09.004

Peer reviewed

HHS Public Access

Author manuscript

Differentiation. Author manuscript; available in PMC 2019 September 19.

Published in final edited form as:

Differentiation. 2018 ; 103: 100–119. doi:10.1016/j.diff.2018.09.004.

Immunohistochemical expression analysis of the human fetal lower urogenital tract

Joel Shen[a,b], **Dylan Isaacson**[a,b], **Mei Cao**[a,b], **Adriane Sinclair**[a,b], **Gerald R. Cunha**[a,b], and **Laurence Baskin**[a,b,*]

[a]Department of Urology, University of California, San Francisco, San Francisco, CA, United States

[b]Division of Pediatric Urology, University of California San Francisco Benioff Children's Hospital, San Francisco, CA, United States

Abstract

We have studied the ontogeny of the developing human male and female urogenital tracts from 9 weeks (in-different stage) to 16 weeks (advanced sex differentiation) of gestation by immunohistochemistry on mid-sagittal sections. Sixteen human fetal pelvises were serial sectioned in the sagittal plane and stained with antibodies to epithelial, muscle, nerve, proliferation and hormone receptor markers. Key findings are: (1) The corpus cavernosum in males and females extends into the glans penis and clitoris, respectively, during the ambisexual stage (9 weeks) and thus appears to be an androgen-independent event. (2) The entire human male (and female) urethra is endodermal in origin based on the presence of FOXA1, KRT 7, uroplakin, and the absence of KRT10 staining. The endoderm of the urethra interfaces with ectodermal epidermis at the site of the urethral meatus. (3) The surface epithelium of the verumontanum is endodermal in origin (FOXA1-positive) with a possible contribution of Pax2-positive epithelial cells implying additional input from the Wolffian duct epithelium. (4) Prostatic ducts arise from the endodermal (FOXA1-positive) urogenital sinus epithelium near the verumontanum. (5) Immunohistochemical staining of mid-sagittal and para-sagittal sections revealed the external anal sphincter, levator ani, bulbospongiosus muscle and the anatomic relationships between these developing skeletal muscles and organs of the male and female reproductive tracts. Future studies of normal human developmental anatomy will lay the foundation for understanding congenital anomalies of the lower urogenital tract.

Keywords

Immunohistochemical; Human fetal lower urogenital tract; Sagittal sections

1. Introduction

The development of the human fetal lower urogenital tract involves the intimate anatomic pairing of the reproductive and urinary systems. The lower urinary tract consists of the

*Correspondence to: Chief Pediatric Urology UCSF Benioff Children's Hospitals, University of California, San Francisco, Department of Urology, 550 16th St, 5th Floor, Mission Hall Pediatric Urology, San Francisco, CA 94158, United States., Laurence.baskin@ucsf.edu (L. Baskin).

bladder, ureters and urethra. The male reproductive tract (minus the gonads) consists of the penis, prostate, seminal vesicles, bulbourethral glands, vas deferens and epididymis, while the female reproductive tract consists of the clitoris, vagina, cervix, uterus and uterine tubes. Development of the bladder and ureters is virtually identical in males and females (see Shen et al., 2018; Isaacson et al., 2018). In contrast, the reproductive tract differentiates into divergent external and internal structures based on the presence of either a testis (androgens and Müllerian inhibiting substance [MIS]) or ovary (absence of androgens and MIS) during critical developmental periods (Baskin et al., 2018; Yamada et al., 2003).

Male and female external genitalia develop from the following primordia: (a) the genital tubercle and (b) the labioscrotal swellings. Human male and female genital tubercles are initially identical in size and morphology. In males the genital tubercle is the primordium of the penis, while in females the genital tubercle is the primordium of the clitoris. The profound differences between clitoral versus penile size and morphology in humans has been attributed to androgen action (Shen et al., 2018, 2016; Baskin et al., 2018; Wilson et al., 1995, 1981; Overland et al., 2016). However, in humans and other species it has become apparent that certain aspects of penile development are androgen-independent (Cunha et al., 2014; Li et al., 2015; Sinclair et al., 2017a).

Until recently our knowledge of the morphogenesis of the human penis and clitoris has been fairly rudimentary and for the most part is based upon simple morphological analyses. Our recent multi-disciplinary studies have demonstrated that the morphogenetic mechanisms of human penile urethral development differ substantially in the shaft versus the glans (Liu et al., 2018b; Li et al., 2015; Shen et al., 2016). Within the penile shaft urethral development involves (a) canalization of the urethral plate (opening zipper) to form an open urethral groove and (b) subsequent fusion of the urethral folds (closing zipper) to form the tubular urethra. In contrast, in the glans penis the urethra forms via direct canalization of the urethral plate without formation of an open urethral groove (Liu et al., 2018a; Baskin et al., 2018). In females the vestibular plate (homologue of the urethral plate in males) canalizes (opening zipper) in a fashion similar to that of the male to form an open vestibular groove (Overland et al., 2016; Baskin et al., 2018), but closure of the vestibular groove (closing zipper) does not occur, presumably due to the absence of androgens. Given that the opening zipper mechanism is common to both sexes, we have proposed that this process is androgen-independent. The closing zipper mechanism is unique to normal males and to females with abnormally elevated androgens during development (congenital adrenal hyperplasia). Congenital adrenal hyperplasia results from impaired cortisol synthesis leading to an increase in androgen production, which in the most severe cases can result in development of normal penile morphology (Speiser et al., 2010).

From a molecular mechanistic perspective, there is considerable evidence for a role of androgens in penile development, while the absence of androgens in normal females or an absence of androgen action secondary to defects in the genes encoding the androgen receptor or 5α-reductase is associated with varying degrees of feminization of the external genitalia (Kim et al., 2002; Wilson et al., 1993, 2011). The expression of androgen receptors in the developing human male and female genital tubercles is consistent with masculinization of the external genitalia. A role for estrogens in development of the external

genitalia has been proposed but is controversial (Zheng et al., 2015; Hutson et al., 2014). Mutant male mice lacking either ESR1 or ESR2 exhibit remarkably normal penile development (Cunha and Sinclair, unpublished). Considerable evidence in animal models demonstrates that exogenous estrogens have teratogenic effects on development of male and female external genitalia (Sinclair et al., 2016a, b; Kim et al., 2004; Mahawong et al., 2014a, b).

The upper portions of male and female reproductive tracts develop from the Wolffian ducts in males and Müllerian ducts in females. In males, the Wolffian ducts form the seminal vesicles, vas deferens and epididymis (Jost et al., 1973). In females the Müllerian ducts form the uterus, cervix and uterine tubes, whereas the vagina arises from urogenital sinus epithelium in humans (Cunha et al., 2018a; Robboy et al., 2017; Bulmer, 1957).

The bladder arises from the urogenital sinus which is endodermal in origin (Liaw et al., 2018). The urethra of the human male and female extends caudally through the pelvis and is continuous with the urethral (and vestibular) plate within the developing genital tubercle. The consensus based upon studies in human and mouse is that the urethral plate (like that of the urethra with which it is continuous) is derived from endoderm (Baskin et al., 2018; Grieshammer et al., 2008; Seifert et al., 2008; Robboy et al., 2017). The endodermal origin of the urethral plate in mice is based upon cell lineage studies in transgenic mice using promoters of sonic hedgehog and Osr1 to target LacZ (Grieshammer et al., 2008; Seifert et al., 2008). The germ layer origin of the human urethral plate, vestibular plate, fetal urethra and introitus in female fetuses has been inferred through the immunohistochemical detection of *FOXA1*, an endodermal associated marker (Robboy et al., 2017; Cunha et al., 2018a).

A current deficiency regarding development of human male and female reproductive tract organs and ductal structures concerns epithelial and mesenchymal differentiation markers of these structures and how these markers relate to the divergent developmental events in human male and female fetal reproductive tract development. Information on the ontogeny of epithelial and mesenchymal differentiation markers will surely advance our understanding of the morphogenetic events in the development of human male and female reproductive tracts

To address this issue we have carried out immunohistochemistry (IHC) for cytokeratins 6, 7, 10, 19 (Baskin et al., 1996; Kurzrock et al., 1999), FOXA1 (Bernardo and Keri, 2012), uroplakin (Sun et al., 1996, 1999), Pax2 (Robboy et al., 2017) S100 for nerves (Baskin et al., 1998), smooth muscle alpha actin and *SM-MHC2* for smooth muscle and myosin heavy chain for skeletal muscle (MHC) (Li et al., 2006; Shiroyanagi et al., 2007; Skrtic et al., 2011). Cellular proliferation was explored through expression of KI67 (Li et al., 2015). The distribution of androgen receptor (AR) and estrogen receptor (ER) was also documented (Qiao et al., 2012a, b). We studied the ontogeny of the developing human male and female urogenital tracts from 9 weeks (in-different stage) to 16 weeks (advanced sex differentiation). This compendium of IHC stains in part provides a molecular basis for understanding the morphogenetic events in development of the human fetal lower urogenital tract. The unique feature of this paper is the extensive use of mid-sagittal sections of human

fetal urogenital tracts that permit observation of the entire urogenital tract from cranial to caudal in which anatomical relationships of the organs are preserved.

2. Methods

Intact first and early second trimester lower human fetal urogenital tracts were collected without patient identifiers after elective termination of pregnancy with approval from the Committee on Human Research at UCSF (IRB#12–08813). Fetal age was estimated using heel-toe length (Drey et al., 2005). Note, that we report age from time of fertilization and not from last menstrual period. Gender was determined using PCR to detect X and Y-chromosomal sequences as previously described (Li et al., 2015) and, when possible, was confirmed by identification of Wolffian and Müllerian duct morphology using a dissecting microscope. Eight to 16-week human fetal male and female specimens were processed for immunofluorescent and immunohistochemical staining.

Sixteen intact human fetal pelvises were acquired and serially sectioned sagittally at 6 μm in the mid-sagittal plane. Every 20th section was stained with hematoxylin and eosin to assess morphology. Intervening sections were processed for immunohistochemistry or immunofluorescence with the following primary antibodies (Table 1). An additional 14 human fetal reproductive tracts were sectioned transversely and processed for immunofluorescent and immunohistochemical staining. Penile measurements were made using the measurement tool in Photoshop, taken from body wall to tip of the glans.

3. Results

3.1. Gross overview of male and female pelvic organs

Fig. 1 depicts human fetal urogenital organs from 9 to 16 weeks fetal age as intact pelvic specimens. In male pelvic specimens, the following structures can be seen: rectum, bladder, prostate, and penis. Dissection is required to more precisely reveal all male urogenital tract organs (Baskin et al., 2018; Cunha et al., 2018b) To obtain mid-sagittal sections further dissection was omitted so as to avoid disturbance of anatomical relationships between the pelvic organs. The bladder is easily identified in all male and female gross specimens (Fig. 1). The urethra begins at the bladder neck (Cunha et al., 2018b; Liaw et al., 2018), which was rarely identified in these gross pelvic specimens. The prostate (rarely seen in these gross specimens) is located below the bladder and encloses the prostatic urethra (Cunha et al., 2018b). The penile urethra terminates distally in the developing penis (Baskin et al., 2018). Given the readily identified landmarks of the path from the bladder to the tip of the penis, the positions of hidden structures can be inferred. The prostate is characterized as a distinct bulge below the male bladder neck (Cunha et al., 2018b); however, it is hidden from view in these gross pelvic specimens underneath layers of connective tissue surrounding this area.

Female pelvic specimens (on the right) reveal the rectum, ovaries, uterine tubes (Müllerian ducts), the upper aspect of the uterovaginal canal, bladder, and clitoris. Further dissection is required to reveal the full extent of the uterovaginal canal (the fused Müllerian ducts) and its caudal attachment to the urethra in the region of the future introitus (vaginal vestibule) (Robboy et al., 2017; Cunha et al., 2018a). Even in fully dissected specimens boundaries

within the uterovaginal canal between the uterine corpus, uterine cervix and vagina are indistinct (Cunha et al., 2018a; Robboy et al., 2017). The anatomical positions of the rectum, bladder, and ureters are equivalent in both sexes. The ureters insert dorsolaterally into the trigone of the bladder to form the ureterovesical junction (Liaw et al., 2018). Note the difference in orientation (angulation) of the penis versus the clitoris. The development of the bipotential genital tubercle at 9 weeks begins by pointing in the caudal direction. At 12 weeks and thereafter in males, the penis has rotated 90 degrees extending prominently from the body wall. The clitoris remains oriented in the caudal direction and in time becomes buried by the developing labia.

3.2. Nine to ten-week male specimens

From a purely morphological perspective, mid-sagittal sections of a 9-week male pelvis reveal several important anatomical features (Fig. 2). The male genital tubercle measures 1.5 mm in length and was pointed in the caudal direction. The bladder upon transition into the urethra continues distally to the urethral meatus, which at 9–10 weeks opens into the urethral groove at the base of the genital tubercle close to the perineum (Fig. 2A–B). The genital tubercle contains the corpus cavernosum (CC) (Fig. 2B, E, H), the solid urethral plate (Fig. 2B), glans penis and urethral meatus (Fig. 2B). The rectum was located dorsal to the bladder and ventral to the fetal spine (Fig. 2A). The Wolffian ducts insert high into the urethra just below the bladder (Fig. 2C). The prostate has not yet formed at 9–10 weeks of gestation (Fig. 2), a fact confirmed by transverse sections through the verumontanum (Fig. 3) as described (Cunha et al., 2018b).

Fig. 3 depicts transverse sections through the verumontanum (an elongated dorsal ridge projecting into the urogenital sinus (prostatic urethra)) and rectum of a 10-week male specimen (Cunha et al., 2018b). Three structures open into the urogenital sinus at the apex of the verumontanum: (a) the midline prostatic utricle (Fig. 3B, D, F) formed at least initially by fusion of the Müllerian ducts (b) flanked by the bilateral Wolffian ducts (Fig. 3B, D, F) destined to form the ejaculatory ducts (see also Cunha et al., 2018b).

3.2.1. FOXA1, PAX2, and cytokeratins 6 and 10 in the 9- to 10-week male specimens—

FOXA1, an endodermal marker (Diez-Roux et al., 2011; Besnard et al., 2004; Robboy et al., 2017), was detected at 9–10 weeks in epithelia of the male bladder, pelvic urethra, urethral plate, urethral groove within the genital tubercle, urethra, verumontanum and rectum (Figs. 2A–C, 3A–B) consistent with the endodermal derivation of these structures (Cunha et al., 2018b, c; Robboy et al., 2017). As expected, FOXA1 was not expressed in the epidermis, Wolffian and Müllerian ducts. PAX2, a marker for Müllerian and Wolffian duct epithelium, was detected in the epithelium of the Wolffian duct (Fig. 2C) and was absent in the urethra and bladder (Fig. 2C) confirming previous studies (Paces-Fessy et al., 2012; Kurita, 2010; Cunha et al., 2018b). Cytokeratins 6 (KRT6) and 10 (KRT10) are markers of stratified epithelia, and specifically KRT10 is a marker of terminal differentiation of epidermis (Moll et al., 1982, 2008). Accordingly, KRT10 was localized to the epidermis (Fig. 2A–B) and was absent in all structures derived from endoderm or mesoderm (Figs. 2 and 3). Distinct transition points in epithelia between FOXA1 and K10 expression were notably seen at the interface between the urethra and skin of the perineum

(urethral meatus) and between the anus and perianal skin (Fig. 2B). KRT6 is more broadly expressed in stratified epithelia and was expressed in the epidermis of the developing penis and in epidermis of the perineum as well as in basal epithelial cells of the urethra (Fig. 2F). At 9 weeks of gestation KRT6 was not detected in the bladder, anal canal and rectum, even though KRT6 appears later in gestation in basal cells of the bladder (see below). At 10 weeks of gestation epithelium of the verumontanum exhibited weak expression of KRT6 in basal epithelial cells (Fig. 3C–D).

3.2.2. Cytokeratins 7 and 19 in the 9- to 10-week male specimens—

Cytokeratins 7 (KRT7) and 19 (KRT19) are intermediate filament proteins found in distinctive layers of a variety of epithelia, especially in simple epithelia (Moll et al., 1982, 2008). KRT7 is also prominently expressed in suprabasal and apical cells of urothelium of the adult bladder and urethra (Moll et al., 1982, 2008). At 9–10 weeks of gestation, KRT7 was detected in apical layers of the bladder and urethra (Fig. 2D–F) as well as in luminal cells of the anal canal. Additionally, KRT7 was expressed in epithelia of the penile urethral groove, the urethral plate and the anal canal but was absent in the rectum and epidermis (Fig. 2D–F). At 10 weeks epithelium of the verumontanum exhibited weak expression KRT7 in apical epithelial cells (Fig. 3C–D), while KRT19 was expressed more broadly in epithelia of the verumontanum, rectum, Wolffian ducts and in the prostatic utricle (fused Müllerian ducts) (Fig. 3E–F).

3.2.3. Smooth muscle myosin heavy chain 2 and myosin heavy chain in the 9- to 10-week male specimens—

The fibromuscular walls of adult male reproductive tract organs contain variable amounts of smooth muscle. Various skeletal muscles are also located in close association with urogenital organs. Smooth muscle myosin heavy chain 2 (SM-MHC2), a marker of terminal differentiation of smooth muscle cells, was expressed in the developing detrusor muscle of the bladder and in the ventral aspect of the bladder neck (Fig. 2G–I) at 9–10 weeks. Note that at this stage smooth muscle of the bladder neck was discontinuous with the detrusor muscle and did not fully encircle the pelvic urethra (labeled smooth muscle in Fig. 2I). SM-MHC2 was also expressed strongly in the circular smooth muscle of the rectum, but not in the longitudinal rectal muscle (Figs. 2I & 3G), and not at all in mesenchyme associated with the verumontanum (Fig. 3G). Myosin heavy chain (MHC), a marker unique to myocardium and skeletal muscle (Gauthier et al., 2000; Morkin, 2000), was localized to musculature of the abdominal wall and external anal sphincter but was absent in the bladder neck at 9 weeks (Figs G–I). MHC was also expressed in the levator ani (Fig. 3H).

3.2.4. S100 in the 10-week male specimen—

S100, a marker of neurons and Schwann cells (Vives et al., 2003), was detected in neurons located in mesenchyme peripheral to the verumontanum and in mesenchyme of the rectum at 10 weeks of gestation (Fig. 3E–F).

3.3. Twelve-week male specimens

Advanced morphogenesis/differentiation is seen in the mid-sagittal sections of a 12-week male pelvis that preserve the anatomical relationships of urogenital organs from the bladder

to the tip of the penis (Figs. 4 and 5). Length of the developing penis has increased to 2.4 mm and has rotated 90 degrees to point in the cranial direction. The bladder showed prominent differentiation of the α-actin-reactive detrusor smooth muscle (Figs. 4E, 5A) with the appearance of the prostate (emergence of prostatic buds) below the bladder neck (Fig. 4B, J, L & 5B, D) (see also Cunha et al., 2018b)). The prostate was surrounded by the prostatic neural plexus (Figs. 4L & 5D). The prostate consisted of canalized and uncanalized prostatic buds that extend and branch distally (Fig. 4B & J, 5D) (Cunha et al., 2018b). The prostatic urethra (not shown) continues distally as segments of the membranous and spongy urethra within the developing penis (Fig. 4C & L). The urethral meatus, which at 9 weeks opened at the base of the penis, has "translocated" distally at 12 weeks to the coronal sulcus as a result of distal fusion of the urethral folds (closing zipper) (Baskin et al., 2018; Liu et al., 2018b). The epithelial tag (Fig. 4C, K) seen at the tip of the genital tubercle is an aggregate of epithelial cells subsequently jettisoned during extensive tissue remodeling of the penile glans (see Liu et al., 2018b; Baskin et al., 2018). The preputial lamina (Figs. 4L & 5C, F) was seen only on the dorsal aspect of the glans penis, which indicates that preputial development begins dorsally within the glans as described in detail in Liu et al. in this issue (Liu et al., 2018b). At later stages (14 weeks, see below) the preputial lamina grows ventrally to eventually completely encircle the glans as described in this issue (Liu et al., 2018b). At 12 weeks the corpus cavernosum was a prominent structure extending from the inferior aspect of the pubic arch into the penile shaft dorsal to the urethra and terminating at the glans (Fig. 4C, L & 5B–C, E–F). The spongy urethra within the developing penis was enclosed by the corpus spongiosum (Fig. 4C–D, L & 5C, E, H), and the bulbospongiosus muscle was seen below the spongy urethra and in the perineum (Fig. 4L).

3.3.1. FOXA1 and cytokeratins 6 and 10 in the 12-week male specimen—

FOXA1 was expressed in epithelia of the bladder, prostatic ducts, pelvic and penile urethras (Fig. 4A–D) and rectum (not illustrated), all known to be derived from endoderm (Cunha et al., 2018c; Robboy et al., 2017) but was not detected in the epidermis and in the epithelial tag (Fig. 4C). At 12 weeks, KRT6 was detected in a few, scattered basal epithelial cells of the bladder (Fig. 4I) and was globally expressed in basal epithelial cells of the urethra (Fig. 4K). KRT6 was also found in basal epithelial cells of solid and canalized prostatic ducts (Fig. 4J), as well as in epithelial cells of the urethral meatus, urethral plate (Fig., 6 (Liu et al., 2018b)), epidermis (Fig. 4K) and anus (not illustrated). The epithelial tag at the tip of the genital tubercle was also KRT6-positive (Fig. 4K). In contrast, K10 was detected in the epidermis and in the epithelial tag, but not in any other structures/tissues (Fig. 4A–C). KRT6 was expressed in the full epithelial thickness (basal to apical epidermal cells), while KRT10 was expressed in supra-basal, but not basal epidermal cells as reported previously (Moll et al., 1982, 2008). Note the sharp interface between FOXA1-positive and KRT10-positive epithelial cells at the urethral meatus (Fig. 4C).

3.3.2. Cytokeratin 7 and uroplakin in the 12-week male specimen—

KRT7 is a differentiation marker of superficial bladder epithelial cells (Moll et al., 2008, 1982). KRT7 was expressed in suprabasal and apical epithelial cells of the bladder, urethra, in solid and canalizing prostatic ducts (Fig. 4J), spongy urethra, and urethral meatus (Fig. 4I–K) but was absent in the epidermis (Fig. 4K). Uroplakin, a marker unique to urothelium (Sun et al.,

1999), was detected in epithelia of the bladder and the entire urethra, terminating short of the epithelial cord and epithelial tag (Fig. 5G–I).

3.3.3. α-Actin, smooth muscle myosin heavy chain 2, and myosin heavy chain in the 12-week male specimen—

Smooth muscle α-Actin (an early marker of smooth muscle differentiation) was detected initially in mesenchyme ventral to the developing prostate and in time spreads dorsally (Cunha et al., 2018b). In the present study α-actin was detected in the fibromuscular walls of the bladder, prostate (Cunha et al., 2018b) and rectum/anal canal at 12 weeks of gestation (Fig. 5A–B). α-Actin was also detected in blood vessels, most notably within the corpus cavernosum, corpus spongiosum, and in the glans penis (Fig. 5B–C). The appearance of SM-MHC2 (a terminal differentiation marker of smooth muscle) confirms that the pattern of α−actin staining is in fact indicative of prostatic smooth muscle differentiation, since at 12 weeks SM-MHC2 immunostaining was seen only in ventral prostatic mesenchyme and not dorsally (Fig. 4F–H) (compare with same pattern in Fig. 15 in Cunha et al. (2018b)). The rectum showed two distinct SM-MHC2-reactive smooth muscle layers – an inner circular layer and an outer weakly SM-MHC2-reactive longitudinal layer (Fig. 4G). In contrast, MHC (a skeletal and cardiac muscle marker) was detected in the levator ani muscle near the bladder neck (Fig. 4H). The levator ani develops bilateral to the prostate and attaches to the posterior aspect of the pubic bones, lying between the pubic bones and smooth muscle of the prostate. MHC was also found in the bulbospongiosus and external anal sphincter (not illustrated).

3.3.4. S100 in the 12-week male specimen—

S100 was detected in ganglia and neurons within the fibromuscular wall of the rectum, the prostatic plexus, dorsal nerve of the penis, ventral urethral fold, and glans penis (Fig. 5D–E).

3.4. Fourteen-week male specimens

The 14-week male pelvis showed increased growth of the rectum, bladder, prostate and the penis in conjunction with the cranial-caudal and dorsal-ventral anatomical relationships of these organs (Figs. 6–8). The bladder leads caudally to the prostatic urethra (Fig. 8H) and continues distally through the membranous and spongy urethras into the penis (Fig. 8H). The prostate showed further canalization of the prostatic buds that branch distally (Figs. 6E, 7C, F, N, 8D) (Cunha et al., 2018b). An ejaculatory duct was also seen inserting into the prostatic urethra below the bladder (Figs. 6B, 7K). The epithelial tag at the distal aspect of the developing penis was no longer present. The prepuce and the preputial lamina have now expanded ventral-laterally to envelop the glans (Fig. 7A, D, 8H) as described (Liu et al., 2018b).

3.4.1. FOXA1 and cytokeratins 6 and 10 in the 14-week male specimen—

FOXA1 was detected in epithelia of the bladder and the entire urethra, but not in other tissues. Specifically, the ejaculatory duct was devoid of FOXA1 expression as is appropriate for a Wolffian duct derivative (Fig. 6B). KRT10 was expressed in the epidermis and the preputial lamina within the glans penis (Fig. 6A). KRT6 was detected in the basal epithelial layer of the bladder at 14 weeks, and additionally KRT6 was expressed in epithelia of the urethra, urethral glands, basal cells of canalized prostatic ducts and in the epidermis,

consistent with a broader range of KRT6 expression relative to KRT10 expression (Fig. 6D–F).

3.4.2. Cytokeratin 7 and uroplakin in the 14-week male specimen—Keratin 7 was expressed in the apical epithelial layers of bladder and urethral epithelia, in apical cells of canalized prostatic ducts and in central cells of solid prostatic buds (Fig. 6D–F). Uroplakin was only expressed in epithelia of the bladder and the urethra (Fig. 7M–O).

3.4.3. Androgen receptor, α-actin, SM-MHC2 in the 14-week male specimen—Androgen receptor (AR) was detected strongly in mesenchyme of the prostate, bulbospongiosus, corpus cavernosum, corpus spongiosum and glans penis (Fig. 7B–D & F–H). AR was also found in apical epithelial layers lining the prostatic urethra, canalized prostatic ducts, and spongy urethra (see Figs. 11–16 in Cunha et al. (2018b)). Bladder epithelium and stroma were AR-negative (Fig. 7A & E). Smooth muscle α-actin, an early marker of smooth muscle differentiation, was detected in fibromuscular walls of the bladder, prostate, rectum, and in blood vessels of the bladder lamina propria, bulbospongiosus, corpus cavernosum, and corpus spongiosum (Fig. 7I–L). In contrast, SM-MHC2 was detected in smooth muscle of the bladder, prostate, and rectum, but not in the penis (Fig. 7J–L). SM-MHC2-positive smooth muscle of the prostate remained localized to ventral mesenchyme and did not fully encircle the prostatic urethra.

3.4.4. S100 in the 14-week male specimen—*S100-reactive nerves were detected in the prostate, the penile shaft and the penile glans (Figs. D-F).* S100-positive neurons were detected most prominently in the penile shaft (dorsal nerve of the penis), in the penile glans and in mesenchyme associated with the prostate (prostatic plexus) (Fig. 7D–F).

3.4.5. Ki67 in the 14-week male specimen—Ki67, a marker for cellular proliferation, was detected ubiquitously in all pelvic organs, but most notably in mesenchymal nuclei associated with the corpus cavernosum (Fig. 8A) and bulbospongiosus (Fig. 8C). Ki67 was also expressed strongly in epithelia of the ejaculatory duct (Fig. 8F), prostatic ducts (Fig. 8F), spongy urethra (Fig. 8B) and anal crypts (Fig. 8G). Note that prostatic ducts shows a gradual increase in Ki67 expression towards the distal aspect of elongating prostatic ducts (Fig. 8D) as described (Cunha et al., 2018b).

3.5. Sixteen-week male specimens

The mid-sagittal sections of the 16-week male pelvis show progressive organ growth compared to the younger specimens and emphasizes anatomical relationships. The penis length has increased to 5.5 mm.

3.5.1. FOXA1 and cytokeratins 6 and 10 in the 16-week male specimen—The expression of FOXA1 is well visualized in urothelium of the bladder, bladder neck, prostatic urethra and penile urethra within the corpus spongiosum (Fig. 9A–C). KRT7 mirrors the expression of FOXA1 in the bladder and urethra (Fig. 9 J–K). At 16 weeks, uniform KRT6 reactivity was observed in basal epithelial cells of the bladder and the urethra as well as in basal cells of prostatic ducts (Fig. 9J–K).

3.5.2. Cytokeratin 7 and uroplakin in the 16-week male specimen—At 16 weeks KRT7 and uroplakin were co-expressed in suprabasal and apical epithelial cells of the bladder and urethra (Fig. 9 J–L and 10 M–P).

3.5.3. Smooth muscle myosin heavy chain 2, α−actin and myosin heavy chain in the 16-week male specimen—Smooth muscle SM-MHC2 was detected in the bladder and rectum. In addition, SM-MHC2-positive smooth muscle fully encircled the spongy urethra below the prostate at 16 weeks (Fig. 9E–F). α-Actin was expressed in the fibromuscular walls of the bladder, prostate, rectum, and in blood vessels of the bladder lamina propria, bulbospongiosus, corpus cavernosum, and corpus spongiosum (Fig. 10 I–L). The MHC-reactive levator ani was located ventral to the smooth muscle of the prostate and attached anteriorly to the pubic bones (Fig. 9E–F). MHC was also found in the bulbospongiosus, perineal muscle, and external anal sphincter (Fig. 9G).

3.5.4. S100 in the 16-week male specimen—S100-positivity was observed in the dorsal nerve of the penis and in nerves within the corpus cavernosum, rectum and bladder (Fig. 9H–I).

3.5.5. Androgen receptor in the 16-week male specimen—Androgen receptor was detected strongly in mesenchyme associated with the prostate, corpus cavernosum, corpus spongiosum, and glans penis, but was absent in the bladder epithelium and stroma and in the epithelial preputial lamina within the penile glans (Fig. 10A–H).

3.6. Ten-week female specimen

Fig. 11 shows transverse sections of a 10-week female pelvis in two regions, cranial and caudal. The caudal sections (Fig. 11A, C & E) are situated below the junction of the uterovaginal canal with the urethra, and thus the uterovaginal canal is not seen. The cranial sections (Fig. 11B, D, & F) contain the uterovaginal canal (fused Müllerian ducts) flanked bilaterally by Wolffian ducts. The rectum and anus are seen in Fig. 11B–F, and the bladder is seen in Fig. 11B, D, & F.

3.6.1. FOXA1, cytokeratin 6, 7, SM-MHC2, MHC in the 10-week female specimen—At 10 weeks, FOXA1, an endodermal marker, was exclusively detected in epithelia of the bladder, urethra, rectum, and anal canal (Fig. 11A–C), but not in the reproductive tract (Wolffian duct, uterovaginal canal, Müllerian ducts) or the epidermis. Taken together, the pattern of FOXA1 expression was consistent with the known endodermal derivation of bladder, urethra, rectum, and anal canal as discussed above. KRT6 was strongly expressed in epidermis (Fig. 11C) and weakly expressed in the basal epithelial cells of the pelvic urethra (not illustrated) and in the anus (Fig. 11C). Epithelia of the bladder, uterovaginal canal (fused Müllerian ducts), and rectum were KRT6 negative (Fig. 11C–D). In contrast, KRT7 was strongly expressed in apical epithelial cells of the bladder (Fig. 11D) decreasing in intensity in urethral epithelium (Fig. 11C). KRT7 was also weakly expressed in apical epithelial cells of the anus but was absent in the rectal epithelium (Fig. 11C–D). SM-MHC2-reactive smooth muscle was found in the detrusor muscle of the bladder (Fig. 11F) and in smooth muscle encircling the rectum (Fig. 11E–F). In contrast, MHC, a marker

of skeletal muscle, was only detected in the levator ani muscle flanking the rectum and urethra (Fig. 11E). The reproductive tract showed no immuno-reactivity to SM-MHC2 or MHC at 10 weeks of gestation (Fig. 11E–F).

3.7. Twelve to sixteen-week female specimens

Figs. 12–15 show mid-sagittal sections of female pelvic organs from 12 to 16 weeks fetal age. The female urogenital organs consist of the uterovaginal canal, bladder, urethra and external genitalia. The anatomical landmarks demarcating the boundaries of the uterus corpus, uterine cervix and vagina cannot be distinguished at these stages in development (Cunha et al., 2018a; Robboy et al., 2017). However, at 12 weeks the solid vaginal plate can be seen at the caudal end of the uterovaginal canal, which joins the urethra at the introitus (Fig. 12H, L, M, 13H, J, K & 14B, K, M) as demonstrated previously (Cunha et al., 2018a; Robboy et al., 2017).

3.8. Twelve-week female specimens

3.8.1. FOXA1 and cytokeratin 10 in the 12-week female specimen—FOXA1 was detected in epithelia of the bladder (Fig. 12A), urethra, introitus, and vestibular groove (Fig. 12C), but was absent in the uterovaginal canal (Fig. 12B) and the solid vaginal plate (which at this stage is composed of Müllerian epithelium) (Cunha et al., 2018a; Robboy et al., 2017). However, at higher magnification, the caudal-most portion of the vaginal plate exhibited FOXA1 staining that was continuous with that of the urethra and introitus (See Fig. 11 in Cunha et al. (2018a) and Robboy et al. (2017)). In contrast, K10 was expressed exclusively in the epidermis and preputial lamina of the glans clitoris (Fig. 12C).

3.8.2. Cytokeratins 6 and 7 in the 12-week female specimen—Similar to the male, KRT6 was observed in the bladder as a discontinuous layer of basal epithelial cells at 12 weeks, whose lumen was lined by KRT7-reactive epithelial cells (Fig. 12G). KRT6 was also weakly expressed in the urethra but was strongly reactive in the most caudal segment of the vaginal plate and introitus (Fig. 12H). KRT7 was detected in epithelia of the uterus, cervix (not shown), vaginal plate, bladder, urethra, and introitus (Fig. 12H).

3.8.3. Smooth muscle myosin heavy chain 2 and myosin heavy chain in the 12-week female specimen—SM-MHC2 expression was detected in smooth muscle of the bladder and rectum, and absent in the reproductive tract (Fig. 12D–E). Circular smooth muscle of the bladder extended distally into the ventral aspect of the bladder neck (Fig. 12E–F). MHC was found in the levator ani that was attached anteriorly to the pubic bones (Fig. 12E–F).

3.8.4. Estrogen receptor α, androgen receptor, uroplakin in the 12-week female specimen—At 12 weeks, estrogen receptor α (ESR1), the dominant receptor for estrogen, was detected strongly in the mesenchyme uterine corpus/uterine cervix, most prominently in the prospective endometrial stroma, but apparently also in regions destined to form myometrium (Fig. 12I). The epithelium of the uterine corpus/uterine cervix was ESR1-negative as described previously (Cunha et al., 2017b). Epithelium of the uterine tube was strongly ESR1-positive (not illustrated, see Cunha et al., 2017b) and was surrounded by

stroma containing ESR1-positive and ESR1-negative cells. Conversely, androgen receptor staining was most intense in the mesenchyme associated with the mid-uterovaginal canal and bladder neck (Fig. 12J). Uroplakin was localized to epithelia of the bladder, urethra, and introitus, with no expression within the vaginal plate or the rest of the female internal genitalia (Fig. 12K–L).

3.9. Fourteen-week female specimens

3.9.1. FOXA1 and cytokeratin 10 in the 14-week female specimen—FOXA1 reactivity was localized to epithelia of the bladder, urethra, and introitus, with no expression within the reproductive tract (Fig. 13A–B) (Cunha et al., 2018a). K10 was expressed in the epidermis (Fig. 13B) and preputial lamina within the glans clitoris (not shown).

3.9.2. Cytokeratins 6 and 7 in the 14-week female specimen—Relative to earlier stages, a higher proportion of basal epithelial cells are KRT6-reactive at 14 weeks in the bladder, the urethra and distally in epithelium lining the introitus and vaginal plate (Fig. 13I–J). In many organs a continuous KRT6 basal layer was observed. KRT7 was detected in apical and suprabasal epithelial layers lining the bladder, urethra, and introitus (Fig. 13J).

3.9.3. S100, Estrogen Receptor α, α-Actin, Uroplakin in the 14-week female specimen—S100-positive neurons were detected most notably within the dorsal nerve of the clitoris and in the glans clitoris (Fig. 13C). ESR1 was highly expressed within mesenchyme and epithelium of the uterine tube (Fig. 13F). In the uterine corpus, the epithelium was mostly ESR1-negative (Fig. 13D–E) as described previously (Cunha et al., 2017a, b). α-Actin was detected in smooth muscle of the bladder, bladder neck, uterine myometrium, uterine tube, rectum, and blood vessels (Fig. 13G). Uroplakin was localized to superficial epithelial cells of the bladder (not shown), urethra, and introitus but absent in the solid vaginal plate (Fig. 13H).

3.10. Sixteen-week female specimens

3.10.1. FOXA1 and cytokeratin 10 in the 16-week female specimen—FOXA1 was detected 16-weeks in epithelia of the bladder (Fig. 14A), urethra (Fig. 14B), and vaginal introitus (Fig. 14C), consistent with observations at earlier stages and previous studies (Cunha et al., 2018a; Robboy et al., 2017). FOXA1 was not observed in Müllerian-derived structures (uterine tube, uterine corpus, uterine cervix) (Fig. 14B). Keratin 10 localized exclusively to the epidermis (Fig. 14D) and preputial lamina within the glans clitoris (Cunha et al., 2018a).

3.10.2. Cytokeratins 6 and 7 in the 16-week female specimen—Both KRT6 and KRT7 were detected in epithelia of the bladder (Fig. 14J), urethra (Fig. 14K), and introitus (Fig. 14K–L) with KRT6 localized to basal epithelial cells and KRT7 localized to supra-basal and apical epithelial cells. KRT7 was also expressed in epithelium of the uterine tube (Fig. 14I). K6 expression was also found in the solid vaginal plate (Fig. 14K) and the preputial lamina within the glans clitoris (Fig. 14L).

3.10.3. Smooth muscle myosin heavy chain 2 and myosin heavy chain in the 16-week female specimen—SM-MHC2 was detected in smooth muscle of the rectum (not shown), bladder (Fig. 14E), and bladder neck (Fig. 14F). At 16 weeks, SM-MHC2-positive smooth muscle was found to fully encircle the urethra in the bladder neck (Fig. 14G). MHC was consistently found in the levator ani that attached anteriorly to the pubic bones (Fig. 14H).

3.10.4. α-Actin, S100, uroplakin in the 16-week female specimen—α-Actin was detected in smooth muscle of the uterine tube (Fig. 15C), bladder (Fig. 15A), bladder neck (Fig. B), uterine myometrium (Fig. 15A), rectum (Fig. 15B), and in blood vessels (Fig. 15A–D). S100 was detected in neurons most notably within the dorsal nerve of the clitoris and glans clitoris (Fig. 15D–F). Lastly, uroplakin was localized to epithelia of the bladder, urethra, and introitus (Fig. 15G–I).

3.10.5. Androgen receptor in the developing female clitoris—The androgen receptor was detected in the developing human female genital tubercle at 9 weeks gestation and the developing clitoris at 12.5, 13 and 14.5 weeks (Fig. 16) in similar fashion to the developing male penis (Fig., 7 A–C). Note the strong expression in the corpus cavernosum and glans clitoris. In the 9 week female genital tubercle there is strong localization of the androgen receptor in the mesenchyme below the corpus cavernosum (Fig. 16 A *). Note in (C & C1) that the epithelium of the preputial lamina is androgen receptor-negative, while the adjacent mesenchyme is androgen receptor-positive.

4. Discussion

The salient feature of this paper is the extensive use of immunohistochemistry on mid-sagittal sections of developing human male and female urogenital tracts. These mid-sagittal sections were obtained from undissected fetal pelvic specimens to preserve the anatomical relationships of the various organs that constitute developing human male and female lower urogenital tracts. Data from mid-sagittal sections was augmented with selected immunohistochemical analysis of transverse sections. Another important feature of our study was the analysis of human fetal specimens over the time frame of 9 (ambisexual) to 16 weeks (advanced sex differentiation) when major morphogenetic events are occurring. Our analysis of mid-sagittal sections augments and confirms many of our other studies on human urogenital development based upon histology and/or immunohistochemistry on transverse sections (Kim et al., 2002; Baskin, 1999; Baskin et al., 1998, 1999; Li et al., 2015; Overland et al., 2016; Shen et al., 2016; Robboy et al., 2017; Cunha et al., 2017b, 2018c; Liu et al., 2018a).

Mid-sagittal sections simultaneously highlight the anatomical relationships of developing urogenital organs in the dorsal-ventral axis and more importantly in the cranial-caudal axis. One anatomical feature whose ontogeny was documented via mid-sagittal sections is the corpus cavernosum of the penis, which is initially represented as a distinct longitudinal mesenchymal condensation. This structure was observed as early as 9 weeks (ambisexual stage) of gestation extending from the perineum distally into the ambisexual genital tubercle into the glans. This distal extension of the corpus cavernosum of the penis into the glans is

confirmed in the 12-week specimen (Fig. 4L) and thereafter in the 14- (Fig. 7A & D, 8H) and 16-week (Fig. 9M) penile specimens. In females, the homologous corpus cavernosum of the clitoris can be seen at 9 weeks extending distally into the glans (Fig. 16A) and Baskin et al. (1999). The presence of the anlage (mesenchymal condensation) of the male and female corpora cavernosa at 9 weeks (ambisexual stage) means that emergence and early development of the corpus cavernosum is androgen independent. Canalization of the urethral and vestibular plates (opening zipper mechanism) is common to both sexes, and thus appears to also be an androgen-independent event (Overland et al., 2016; Baskin et al., 2018). Other examples of androgen-in-dependent development of male external genitalia can be found in moles and the spotted hyena (Cunha et al., 2014; Sinclair et al., 2017b). It is noteworthy that mid-sagittal sections are particularly useful for defining the ontogeny of the corpus cavernosum within male and female genital tubercles (and especially the full proximal to distal extent of this structure).

During development of the male urogenital system, *FOXA1* staining is seen consistently in male and female bladders, the urethras (Figs. 2–4 and 9), the fetal verumontanum and prostatic ducts, signifying their derivation from endoderm as described (Cunha et al., 2018b; Robboy et al., 2017). Caudally an interface exists between endoderm and ectoderm at the urethral meatus. In males this endodermal/ectodermal interface “translocates” distally during development as the closing zipper (fusion of the urethral folds) extends distally towards the glans (also see Liu et al., 2018b; Baskin et al., 2018). This endodermal/ectodermal interface is revealed in mid-sagittal sections stained for *FOXA1* (an endodermal marker) and keratin 10, a marker indicative of mature epidermis. While keratin 10 is not strictly an ectodermal marker, the precise coincidence of the FOXA1/keratin 10 interface at the urethral meatus is more than intriguing. At 9 weeks, Fig. 2B shows this endodermal/ectodermal interface to be located proximally at the level of the open urethral groove at the site of the closing zipper. As development proceeds the endodermal/ectodermal interface and the urethral meatus progresses distally. At 12 weeks the urethral meatus has extended distal to the coronal margin (proximal glans) (Fig. 4C). At 14 and 17 weeks (see Fig. 5 Liu et al., 2018b) the *FOXA1*/KRT10 interface (the presumed endodermal/ectodermal interface) is at the urethral meatus near the tip of the penis. Although we have not examined the adult penile urethral meatus with *FOXA1*/KRT10 immunostaining, we suggest based upon these data that the entire human penile urethra is derived from endoderm. Thus, in adulthood we hypothesize that endodermal/ectodermal interface is located at the urethral meatus.

The verumontanum is another site of an interface between epithelia of different germ layers. The consensus from the literature is that the surface epithelium of the verumontanum is endoderm (*FOXA1*-positive), and the ejaculatory ducts opening onto the verumontanum are mesodermal in origin (PAX2-positive) (see review Cunha et al., 2018b). The embryologic origin of the prostatic utricle is controversial. Meyer proposed that the utricle was derived from the fused Müllerian ducts (Meyer, 1909). Shapiro et al. has recently suggested that the prostatic utricle forms as an ingrowth of specialized epithelial cells from the dorsal wall of the urogenital sinus as the caudal Müllerian ducts regress (Shapiro et al., 2004), perhaps in a process similar to that which occurs in human vaginal development (Robboy et al., 2017; Bulmer, 1957). We show that at 9 weeks that Pax2-positive epithelial cells continuous with the Wolffian duct epithelium contribute to surface epithelium of the verumontanum (see Fig.

6 in Cunha et al. (2018b)). Further investigation will be required to elucidate epithelial origin of the verumontanum over a wide developmental time frame.

Prostatic ducts arise from the endodermal (*FOXA1*-positive) urogenital sinus epithelium near the verumontanum (Cunha et al., 2018b). Immunostaining of mid-sagittal sections with antibodies to cytokeratins 6, 7, 19, and the androgen receptor are in complete agreement with our studies on human prostatic development (Cunha et al., 2018b). Solid prostatic ducts emerge from the urogenital sinus, and initially the epithelial cells of solid prostatic buds co-express basal and luminal cells markers (mainly keratins) (Wang et al., 2001). With development epithelial cells of the core of solid prostatic ducts express luminal cell markers such as KRT7 (Fig. 6E), which are in turn surrounded by prospective basal epithelial cells expressing KRT6 (Fig. 6E). Once the ducts canalize, the luminal cells express KRT7 and other luminal cell markers (KRT8, KRT18, androgen receptor) and the definitive basal cells express KRT6 and other basal cell markers (KRT14 and TP63) (Cunha et al., 2018b). S100 immunostaining of mid-sagittal sections revealed the prostatic plexus (Fig. 5) and complement the light sheet immunofluorescent imaging reported in Cunha et al. (2018b). Mid-sagittal sections immunostained for S100 reveal caudal extension of nerve fibers from the prostatic plexus into the developing penis (Figs. 7, 9, 10). Homologous nerve bundles were also seen in the developing clitoris (Figs. 13 and 15). More detailed and more accurate tracing of nerve fibers from the pelvis into the penis and clitoris will be required to fully understand the development of innervation of these organs.

Differentiation of mesenchyme into muscular elements (smooth muscle and skeletal muscle) was also explored in this paper. Previous studies from our laboratory have documented the ontogeny of smooth muscle in the developing female reproductive tract using an antibody to α−actin (Cunha et al., 2018a) in both transverse and mid-sagittal sections. The ontogeny of bladder and prostatic smooth muscle was described based upon α−actin immunostaining (Cunha et al., 2018b). Observations from both of these male and female studies are confirmed and extended through the use of antibodies to SM-MHC2, a marker of terminal smooth muscle differentiation. For the most part the expression of α-actin (an early marker of smooth muscle differentiation) and SM-MHC2 (a late marker of smooth muscle differentiation) were congruent suggesting a rapidly paced process of smooth muscle differentiation. Use of mid-sagittal sections provided additional anatomic information on smooth muscle differentiation in the bladder and prostate. It is interesting that developing prostatic smooth muscle is androgen receptor positive (Cunha et al., 2018b), while the developing myometrium of the uterus appears to be positive for both ESR1 and androgen receptor (Cunha et al., 2017b, 2018a). The developing human prostate was not examined for ESR1, and so the possibility that developing human prostatic smooth muscle is positive for both ESR1 and androgen receptor remains to be determined. Through use of antibodies to α-actin and SM-MHC2 it is evident that the differentiation of smooth muscle occurs on vastly different temporal scales within pelvic organs of males and females. Smooth muscle differentiation within the rectum/anus precedes that in the prostate, bladder, urethra and uterus (Figs. 2, 3, 11). Indeed, in the rectum the circular smooth muscle layer appears well before the longitudinal smooth muscle layer (Fig. 3). Similarly in the mouse and rat uterus, the inner circular myometrial layer appears several days before the outer longitudinal myometrial layer (Brody and Cunha, 1989).

For the first time, the ontogeny of skeletal muscle was explored relative to its association with the developing human male and female urogenital tracts using immunostaining for myosin heavy chain, a known skeletal muscle marker (Soukup et al., 1995). Through use of mid-sagittal and para-sagittal sections we were able to identify the external anal sphincter, levator ani, bulbospongiosus muscle and to appreciate the anatomic relationships between these developing skeletal muscles and organs of the male and female reproductive tracts. Our brief (and incomplete) survey of these developing skeletal muscles requires further study.

The germ layer origin of vaginal epithelium was not specifically addressed in the present study, and for this topic our previous studies should be consulted (Cunha et al., 2018a; Robboy et al., 2017). Historically, Koff's publication in 1933 and Bulmer's in 1957 were the two most important studies on origin of human vaginal epithelium (Bulmer, 1957; Koff, 1933). Both investigators proposed that Müllerian and urogenital sinus epithelia play major roles. Koff asserted that Müllerian epithelium was key, assigning a minor role to urogenital sinus epithelium (UGE) to human vaginal epithelial development. Bulmer stated that UGE upgrowth "forms the whole of (the vaginal) epithelial lining" (Bulmer, 1957). Both studies were based exclusively upon hematoxylin and eosin (H&E) stained sections. Our immunohistochemical studies, using FOXA1 (an endodermal UGE marker) and PAX2 (a Müllerian epithelial marker) confirmed Bulmer's interpretation by showing that UGE of the vaginal plate grows cranially to completely replace the Müllerian epithelium to the level of the cervical os (Robboy et al., 2017). While the present study did not revisit the question of the origin of human vaginal epithelium, the results of our *FOXA1* immunostaining corroborated our earlier studies. It is worth noting that cell lineage tracing and immunohistochemical studies in mice indicate that adult vaginal epithelium is derived exclusively from Müllerian epithelium (Kurita, 2010). Thus, derivation of vaginal epithelium appears to be dramatically different in mice versus humans. Finally, an important observation of our earlier study (Robboy et al., 2017) was that the developing human vaginal introitus is *FOXA1*-positive and thus endodermal in origin. Our present study confirms this interpretation, also implying that the hymen is lined/covered by epithelium of urogenital sinus origin.

In this study we have made extensive use of antibodies to cytokeratins 6, 7, 10 and 19. Cytokeratins are epithelial cytoskeletal proteins organized into intermediate filaments, which resist mechanical stress. Cytokeratins 6 and 10 typically are reactive to stratified epithelia such as epidermis in which KRT10 is expressed in all layers except the basal cell layer. In contrast, KRT6 is reactive to all layers of the epidermis (basal to apical). In the present study KRT10 was only detected in the epidermis, the preputial lamina and the epithelial tag, while KRT6 was detected in the epidermis (and epithelial tag), as well in the basal epithelial cells of the bladder, urethra, and the prostate, confirming previous studies (Cunha et al., 2017b). The expression of KRT10 in the preputial lamina strengthens our interpretation that KRT10 in developing human external genitalia is indicative of the ectodermal lineage. The preputial lamina emerges from a dorsal epidermal thickening on the glans called the preputial placode (Liu et al., 2018b) and therefore is undoubtedly ectodermal in origin. In females, KRT6 was expressed in epithelia of the vaginal plate and definitive vaginal epithelium also confirming previous studies (Cunha et al., 2017b, 2018a). Another important difference in the

expression of KRT6 and KRT10 is that KRT6 is reactive to the fetal urethral (also the vestibular) plate, while KRT10 is not expressed in these structures (see Fig. 5 in Liu et al. (2018b)). Results of the current paper corroborate our earlier studies.

Cytokeratin 7 and 19 are typically expressed in simple epithelia and also in urothelium (Moll et al., 1982, 2008). KRT7 was expressed in suprabasal urothelial cells of the developing human bladder and urethra as well as in epithelial cells of the verumontanum, central core cells and luminal cells of the prostate (Cunha et al., 2018b), epithelial cells of the uterine tube, uterine corpus and endocervix, introitus, and the Müllerian duct (Cunha et al., 2017b, 2018a). Findings in the present study are in complete agreement with these assertions from our previous reports. Through use of mid-sagittal sections, it is notable that at the endodermal/ectodermal (*FOXA1*/KRT10) interface *FOXA1* expression coincides precisely with KRT7 expression at the urethral meatus in males and in the introitus in females. Perfect co-expression of *FOXA1* and KRT7 staining is also seen in the bladder and urethra. Expression of uroplakin is for the most part in concordance with that of *FOXA1* and KRT7 expression.

Androgen receptor is expressed in both developing human male and female lower urogenital tracts, which is consistent with androgen-dependent development and growth of the penis and its internal elements as well as the prostate and prostatic urethra. A similar androgen receptor expression pattern is seen in the developing clitoris as is seen in the penis (Fig. 16). This is consistent with the morphogenetic bipotential growth of the ambisexual human genital tubercle, which can develop into either a penis or clitoris depending on the presence or absence, respectively, as discussed above. The results of the present study corroborate earlier studies (Kim et al., 2002).

Our finding of estrogen receptor in the developing human female lower urogenital tract is in agreement with earlier studies of ESR1 expression in the uterus and uterine tube (Cunha et al., 2017b, 2018a). An interesting finding in both developing male and female urogenital tracts is the apparent co-expression of androgen receptor and ESR1 expression in organs/tissues such as the uterine tube and the myometrium. The developing human prostate expresses both androgen receptor (Cunha et al., 2018b) and estrogen receptors (Adams et al., 2002; Shapiro et al., 2005), but whether these receptors are expressed in the same cell type remains to be determined. In the human fetal penis androgen receptors, ESR1 and ESR2 (Qiao et al., 2012a) are expressed, but more detail is required concerning the cell types expressing these receptors. The role of estrogen in normal development and the development of hypospadias is under investigation (Hutson et al., 2014; Cunha et al., 2015).

In summary, we have performed an immunohistochemical ontogeny on mid-sagittal sections of developing human male and female urogenital tracts from 9 weeks (indifferent stage) to 16 weeks gestation (advanced sexual differentiation). Mid-sagittal sections compliment the other multi-dimensional techniques that have been used to study development of the lower urogenital tracts of human and include: optical projection tomography, scanning electron microscopy, lightsheet fluorescence microscopy and wholemount microscopy. Novel findings and confirmation of previous observations include: (1) The distal extension of the corpus cavernosum in males and females abutting the glans penis and glans clitoris,

respectively. (2) The entire human male (and female) urethra is endodermal in origin based on FOXA1, KRT7, uroplakin, and KRT10 staining. (3) The interface between ectodermal epidermis and endoderm of the urethra occurs at the site of the urethral meatus in males and the introitus in females. (4) The surface epithelium of the verumontanum is endodermal in origin (*FOXA1*-positive) with possible contribution of Pax2-positive Wolffian duct epithelial cells. (5) Prostatic ducts arise from the endodermal (*FOXA1*-positive) urogenital sinus epithelium near the verumontanum. (6) The ontogeny of smooth and skeletal muscle was described, and vast differences were noted in the timing of appearance of smooth muscle in pelvic gastrointestinal organs versus urogenital organs. (7) Anatomic relationships between developing skeletal muscle and organs of the male and female reproductive tracts were described. (8) Using FOXA1 (an endodermal urogenital sinus epithelium marker) and PAX2 (a Müllerian epithelial marker), our data supports previous findings that the urogenital sinus epithelium of the vaginal plate grows cranially to completely replace the Müllerian epithelium to the level of the cervical os thereby forming the epithelium of the human vagina. Future studies of normal developmental human anatomy will lay the foundation for understanding the molecular mechanisms of normal development of human male and female urogenital tract and their congenital anomalies.

Abbreviations:

KRT	keratin
MIS	Müllerian inhibiting substance
AR	androgen receptor
ER	estrogen receptor

References

Adams JY, Leav I, Lau KM, Ho SM, Pflueger SM, 2002 Expression of estrogen receptor beta in the fetal, neonatal, and prepubertal human prostate. Prostate 52, 69–81. [PubMed: 11992621]

Baskin L, Shen J, Sinclair A, Cao M, Liu X, Liu G, Isaacson D, Overland M, Li Y, Cunha J, 2018 Development of the Human Penis and Clitoris. Differentiaiton (In this issue0

Baskin LS, 1999 Fetal genital anatomy reconstructive implications. J. Urol 162, 527–529. [PubMed: 10411082]

Baskin LS, Erol A, Li YW, Cunha GR, 1998 Anatomical studies of hypospadias. J. Urol 160, 1108–1115. [PubMed: 9719287]

Baskin LS, Erol A, Li YW, Liu WH, Kurzrock E, Cunha GR, 1999 Anatomical studies of the human clitoris. J. Urol 162, 1015–1020. [PubMed: 10458423]

Baskin LS, Hayward SW, Young PF, Cunha GR, 1996 Ontogeny of the rat bladder: smooth muscle and epithelial differentiation. Acta Anat 155, 163–171 (Basel). [PubMed: 8870784]

Bernardo GM, Keri RA, 2012 FOXA1: a transcription factor with parallel functions in development and cancer. Biosci. Rep 32, 113–130. [PubMed: 22115363]

Besnard V, Wert SE, Hull WM, Whitsett JA, 2004 Immunohistochemical localization of Foxa1 and Foxa2 in mouse embryos and adult tissues. Gene Expr. Pattern.: GEP 5, 193–208.

Brody JR, Cunha GR, 1989 Histologic, morphometric, and immunocytochemical analysis of myometrial development in rats and mice: I. Normal development. Am. J. Anat 186, 1–20. [PubMed: 2782286]

Bulmer D, 1957 The development of the human vagina. J. Anat 91, 490–509. [PubMed: 13475148]

Cunha G, Robboy S, Kurita T, Isaacson D, Shen J, Cao M, Baskin L, 2018a Development of the human vagina, cervix, uterus and fallopian tube. Differentiation (In this issue)

Cunha G, Vezina C, Isaacson D, Ricke W, Timms B, Baskin L, 2018b Development of the human prostate and seminal vesicle. Differentiation (in this issue)

Cunha GR, Kurita T, Cao M, Shen J, Cooke PS, Robboy SJ, Baskin LS, 2018c Tissue interactions and estrogenic response during human female fetal reproductive tract development. Differentiation 101, 39–45. [PubMed: 29684808]

Cunha GR, Kurita T, Cao M, Shen J, Robboy SJ, Baskin L, 2017a Response of xenografts of developing human female reproductive tracts to the synthetic estrogen, diethylstilbestrol. Differ.; Res. Biol. Divers 98, 35–54.

Cunha GR, Risbridger G, Wang H, Place NJ, Grumbach M, Cunha TJ, Weldele M, Conley AJ, Barcellos D, Agarwal S, Bhargava A, Drea C, Siiteri PK, Coscia EM, McPhaul MJ, Hammond GL, Baskin LS, Glickman SE, 2014 Development of the external Genitalia: perspectives from the spotted hyena (Crocuta crocuta). Differ.; Res. Biol. Divers 87, 4–22.

Cunha GR, Sinclair A, Risbridger G, Hutson J, Baskin LS, 2015 Current understanding of hypospadias: relevance of animal models. Nat. Rev. Urol 12, 271–280. [PubMed: 25850792]

Cunha GR, T, K, Cao M, Shen J, Robboy S, L, B, 2017b Molecular mechanisms of development of the human fetal female reproductive tract. Differentiaiton 97, 54–72.

Diez-Roux G, Banfi S, Sultan M, Geffers L, Anand S, Rozado D, Magen A, Canidio E, Pagani M, Peluso I, Lin-Marq N, Koch M, Bilio M, Cantiello I, Verde R, De Masi C, Bianchi SA, Cicchini J, Perroud E, Mehmeti S, Dagand E, Schrinner S, Nurnberger A, Schmidt K, Metz K, Zwingmann C, Brieske N, Springer C, Hernandez AM, Herzog S, Grabbe F, Sieverding C, Fischer B, Schrader K, Brockmeyer M, Dettmer S, Helbig C, Alunni V, Battaini MA, Mura C, Henrichsen CN, Garcia-Lopez R, Echevarria D, Puelles E, Garcia-Calero E, Kruse S, Uhr M, Kauck C, Feng G, Milyaev N, Ong CK, Kumar L, Lam M, Semple CA, Gyenesei A, Mundlos S, Radelof U, Lehrach H, Sarmientos P, Reymond A, Davidson DR, Dolle P, Antonarakis SE, Yaspo ML, Martinez S, Baldock RA, Eichele G, Ballabio A, 2011 A high-resolution anatomical atlas of the transcriptome in the mouse embryo. PLoS Biol 9, e1000582. [PubMed: 21267068]

Drey EA, Kang MS, McFarland W, Darney PD, 2005 Improving the accuracy of fetal foot length to confirm gestational duration. Obstet. Gynecol 105, 773–778. [PubMed: 15802404]

Gauthier FV, Qadir MA, Merrifield PA, Atkinson BG, 2000 Postembryonic expression of the myosin heavy chain genes in the limb, tail, and heart muscles of metamorphosing amphibian tadpoles. Microsc. Res. Tech 50, 458–472. [PubMed: 10998636]

Grieshammer U, Agarwal P, Martin GR, 2008 A Cre transgene active in developing endodermal organs, heart, limb, and extra-ocular muscle. Genesis 46, 69–73. [PubMed: 18257103]

Hutson JM, Baskin LS, Risbridger G, Cunha GR, 2014 The power and perils of animal models with urogenital anomalies: handle with care. J. Pediatr. Urol 10, 699–705. [PubMed: 24768568]

Isaacson D, Shen J, Overland M, Li Y, Sinclair A, Cao M, McCreedy D, Calvert M, McDevitt T, Cunha GR, Baskin L, 2018 Three-dimensional imaging of the developing human fetal urogenital-genital tract: indifferent stage to male and female differentiation. Differentiaiton (In this issue)

Jost A, Vigier B, Prepin J, Perchellet JP, 1973 Studies on sex differentiation in mammals. Recent Prog. Horm. Res 29, 1–41. [PubMed: 4584366]

Kim KS, Liu W, Cunha GR, Russell DW, Huang H, Shapiro E, Baskin LS, 2002 Expression of the androgen receptor and 5 alpha-reductase type 2 in the developing human fetal penis and urethra. Cell Tissue Res 307, 145–153. [PubMed: 11845321]

Kim KS, Torres CR Jr., Yucel S, Raimondo K, Cunha GR, Baskin LS, 2004 Induction of hypospadias in a murine model by maternal exposure to synthetic estrogens. Environ. Res 94, 267–275. [PubMed: 15016594]

Koff AK, 1933 Development of the Vagina in the human fetus. Contrib. Embryol. Contrib. Embryol 24 Carnegie Inst, Wash, pp. 59–90. [PubMed: 12332362]

Kurita T, 2010 Developmental origin of vaginal epithelium. Differ.; Res. Biol. Divers 80, 99–105.

Kurzrock EA, Baskin LS, Cunha GR, 1999 Ontogeny of the male urethra: theory of endodermal differentiation. Differ.; Res. Biol. Divers 64, 115–122.

Li J, Shiroyanagi Y, Lin G, Haqq C, Lin CS, Lue TF, Willingham E, Baskin LS, 2006 Serum response factor, its cofactors, and epithelial-mesenchymal signaling in urinary bladder smooth muscle formation. Differ.; Res. Biol. Divers 74, 30–39.

Li Y, Sinclair A, Cao M, Shen J, Choudhry S, Botta S, Cunha G, Baskin L, 2015 Canalization of the urethral plate precedes fusion of the urethral folds during male penile urethral development: the double zipper hypothesis. J. Urol 193, 1353–1359. [PubMed: 25286011]

Liaw A, Cunha GR, Cao M, Baskin L, 2018 Development of the bladder and ureterovesical junction. Differentiation (In this issue)

Liu G, Liu X, Shen J, Sinclair A, Baskin L, Cunha GR, 2018a Contrasting mechanisms of penile urethral formation in mouse and human. Differ.; Res. Biol. Divers 101, 46–64.

Liu X, Liu G, Shen J, Isaacson D, Sinclair A, Cao M, Liaw A, Cunha GR, Baskin LS, 2018b Human glans and preputial development. Differentiaiton (In this issue)

Mahawong P, Sinclair A, Li Y, Schlomer B, Rodriguez E Jr., Ferretti MM, Liu B, Baskin LS, Cunha GR, 2014a Comparative effects of neonatal diethylstilbestrol on external genitalia development in adult males of two mouse strains with differential estrogen sensitivity. Differ.; Res. Biol. Divers 88, 70–83.

Mahawong P, Sinclair A, Li Y, Schlomer B, Rodriguez E Jr., Ferretti MM, Liu B, Baskin LS, Cunha GR, 2014b Prenatal diethylstilbestrol induces malformation of the external genitalia of male and female mice and persistent second-generation developmental abnormalities of the external genitalia in two mouse strains. Differ.; Res. Biol. Divers 88, 51–69.

Meyer R, 1909 Zur entwicklungsgeschichte und anatomie des utriculus prostaticus beim menschen. Arch. Mikrosk. Anat 74, 844.

Moll R, Divo M, Langbein L, 2008 The human keratins: biology and pathology. Histochem Cell Biol 129, 705–733. [PubMed: 18461349]

Moll R, Franke WW, Schiller DL, Geiger B, Krepler R, 1982 The catalog of human cytokeratin polypeptides: patterns of expression of specific cytokeratins in normal epithelia, tumors, and cultured cells. Cell 31, 11–24. [PubMed: 6186379]

Morkin E, 2000 Control of cardiac myosin heavy chain gene expression. Microsc. Res. Tech 50, 522–531. [PubMed: 10998641]

Overland M, Li Y, Cao M, Shen J, Yue X, Botta S, Sinclair A, Cunha G, Baskin L, 2016 Canalization of the vestibular plate in the absence of urethral fusion characterizes development of the human clitoris: the single zipper hypothesis. J. Urol 195, 1275–1283. [PubMed: 26926534]

Paces-Fessy M, Fabre M, Lesaulnier C, Cereghini S, 2012 Hnf1b and Pax2 cooperate to control different pathways in kidney and ureter morphogenesis. Hum. Mol. Genet 21, 3143–3155. [PubMed: 22511595]

Qiao L, Rodriguez E Jr., Weiss DA, Ferretti M, Risbridger G, Cunha GR, Baskin LS, 2012a Expression of estrogen receptor alpha and beta is decreased in hypospadias. J. Urol 187, 1427–1433. [PubMed: 22341273]

Qiao L, Tasian GE, Zhang H, Cao M, Ferretti M, Cunha GR, Baskin LS, 2012b Androgen receptor is overexpressed in boys with severe hypospadias, and ZEB1 regulates androgen receptor expression in human foreskin cells. Pediatr. Res 71, 393–398. [PubMed: 22391641]

Robboy SJ, Kurita T, Baskin L, Cunha GR, 2017 New insights into human female reproductive tract development. Differentiation 97, 9–22. [PubMed: 28918284]

Seifert AW, Harfe BD, Cohn MJ, 2008 Cell lineage analysis demonstrates an endodermal origin of the distal urethra and perineum. Dev. Biol 318, 143–152. [PubMed: 18439576]

Shapiro E, Huang H, Masch RJ, McFadden DE, Wilson EL, Wu XR, 2005 Immunolocalization of estrogen receptor alpha and beta in human fetal prostate. J. Urol 174, 2051–2053. [PubMed: 16217392]

Shapiro E, Huang H, McFadden DE, Masch RJ, Ng E, Lepor H, Wu XR, 2004 The prostatic utricle is not a Mullerian duct remnant: immunohistochemical evidence for a distinct urogenital sinus origin. J. Urol 172, 1753–1756 (discussion 1756). [PubMed: 15371806]

Shen J, Cunha G, Sinclair A, Cao M, Isaacson D, Baskin L, 2018 Macroscopic whole-mounts of the developing human fetal urogenital-genital tract: indifferent stage to male and female differentiation. Differentiation (In this issue)

Shen J, Overland M, Sinclair A, Cao M, Yue X, Cunha G, Baskin L, 2016 Complex epithelial remodeling underlie the fusion event in early fetal development of the human penile urethra. Differentiation 92, 169–182. [PubMed: 27397682]

Shiroyanagi Y, Liu B, Cao M, Agras K, Li J, Hsieh MH, Willingham EJ, Baskin LS, 2007 Urothelial sonic hedgehog signaling plays an important role in bladder smooth muscle formation. Differentiation 75, 968–977. [PubMed: 17490411]

Sinclair AW, Cao M, Baskin L, Cunha GR, 2016a Diethylstilbestrol-induced mouse hypospadias: "window of susceptibility". Differ.; Res. Biol. Divers 91, 1–18.

Sinclair AW, Cao M, Pask A, Baskin L, Cunha GR, 2017a Flutamide-induced hypospadias in rats: a critical assessment. Differ.; Res. Biol. Divers 94, 37–57.

Sinclair AW, Cao M, Shen J, Cooke P, Risbridger G, Baskin L, Cunha GR, 2016b Mouse hypospadias: a critical examination and definition. Differentiation 92, 306–317. [PubMed: 27068029]

Sinclair AW, Glickman S, Catania K, Shinohara A, Baskin L, Cunha GR, 2017b Comparative morphology of the penis and clitoris in four species of moles (Talpidae). J. Exp. Zool. B Mol. Dev. Evol 328, 275–294. [PubMed: 28251823]

Skrtic A, Sokolic L, Borovecki A, Rosa J, Fenzl V, 2011 Immunohistochemical localization of CD31, NOTCH1 and JAGGED1 proteins in experimentally induced polycystic ovaries of immature rats. Acta Histochem 113, 262–269. [PubMed: 19932502]

Soukup T, Pedrosa-Domellof F, Thornell LE, 1995 Expression of myosin heavy chain isoforms and myogenesis of intrafusal fibres in rat muscle spindles. Microsc. Res. Tech 30, 390–407. [PubMed: 7787238]

Speiser PW, Azziz R, Baskin LS, Ghizzoni L, Hensle TW, Merke DP, Meyer-Bahlburg HF, Miller WL, Montori VM, Oberfield SE, Ritzen M, White PC, Endocrine S, 2010 Congenital adrenal hyperplasia due to steroid 21-hydroxylase deficiency: an Endocrine Society clinical practice guideline. J. Clin. Endocrinol. Metab 95, 4133–4160. [PubMed: 20823466]

Sun TT, Liang FX, Wu XR, 1999 Uroplakins as markers of urothelial differentiation. Adv. Exp. Med. Biol 462, 7–18 (discussion 103–114). [PubMed: 10599409]

Sun TT, Zhao H, Provet J, Aebi U, Wu XR, 1996 Formation of asymmetric unit membrane during urothelial differentiation. Mol. Biol. Rep 23, 3–11. [PubMed: 8983014]

Vives V, Alonso G, Solal AC, Joubert D, Legraverend C, 2003 Visualization of S100B-positive neurons and glia in the central nervous system of EGFP transgenic mice. J. Comp. Neurol 457, 404–419. [PubMed: 12561079]

Wang Y, Hayward S, Cao M, Thayer K, Cunha G, 2001 Cell differentiation lineage in the prostate. Differ.; Res. Biol. Divers 68, 270–279.

Wilson JD, George FW, Griffin JE, 1981 The hormonal control of sexual development. Science 211, 1278–1284. [PubMed: 7010602]

Wilson JD, George FW, Renfree MB, 1995 The endocrine role in mammalian sexual differentiation. Recent Progress. Horm. Res 50, 349–364.

Wilson JD, Griffin JE, Russell DW, 1993 Steroid 5 alpha-reductase 2 deficiency. Endocr. Rev 14, 577–593. [PubMed: 8262007]

Wilson JM, Arnhym A, Champeau A, Ebbers M, Coakley F, Baskin L, 2011 Complete androgen insensitivity syndrome: an anatomic evaluation and sexual function questionnaire pilot study. J. Pediatr. Urol 7, 416–421. [PubMed: 20719566]

Yamada G, Satoh Y, Baskin LS, Cunha GR, 2003 Cellular and molecular mechanisms of development of the external genitalia. Differ.; Res. Biol. Divers 71, 445–460.

Zheng Z, Armfield BA, Cohn MJ, 2015 Timing of androgen receptor disruption and estrogen exposure underlies a spectrum of congenital penile anomalies. Proc. Natl. Acad. Sci. USA 112, E7194–E7203. [PubMed: 26598695]

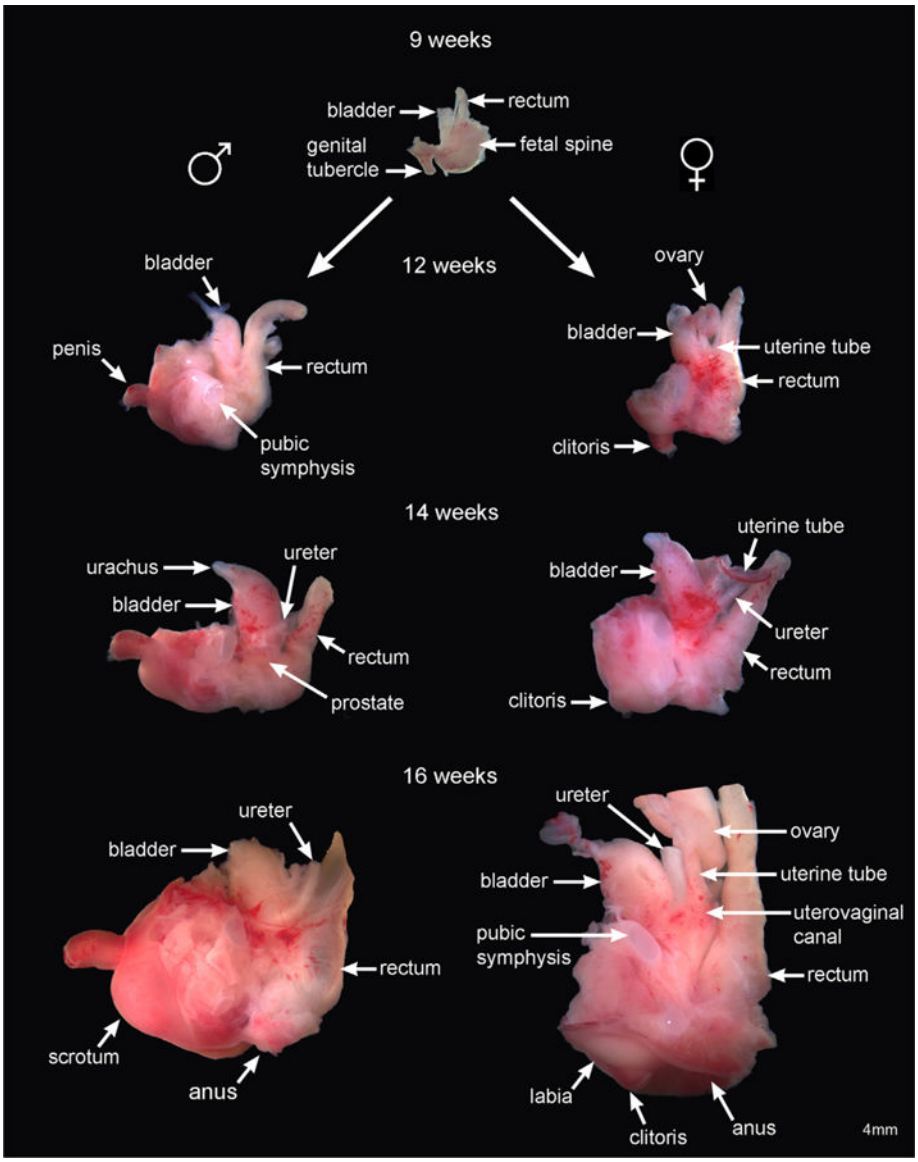

Fig. 1.

Depicts development of human fetal pelvic organs from 9 (indifferent stage) to 16 weeks fetal age. Male urogenital structures shown on the left consists of the bladder, prostate, and penis. Female urogenital structures shown on the right consists of the ovaries, reproductive tract (uterine tubes and uterovaginal canal), bladder and clitoris. Note that at 12 weeks and thereafter in the male, the penis has rotated 90 degrees extending prominently from the body wall. The female clitoris, in contrast, remains oriented in the caudal direction.

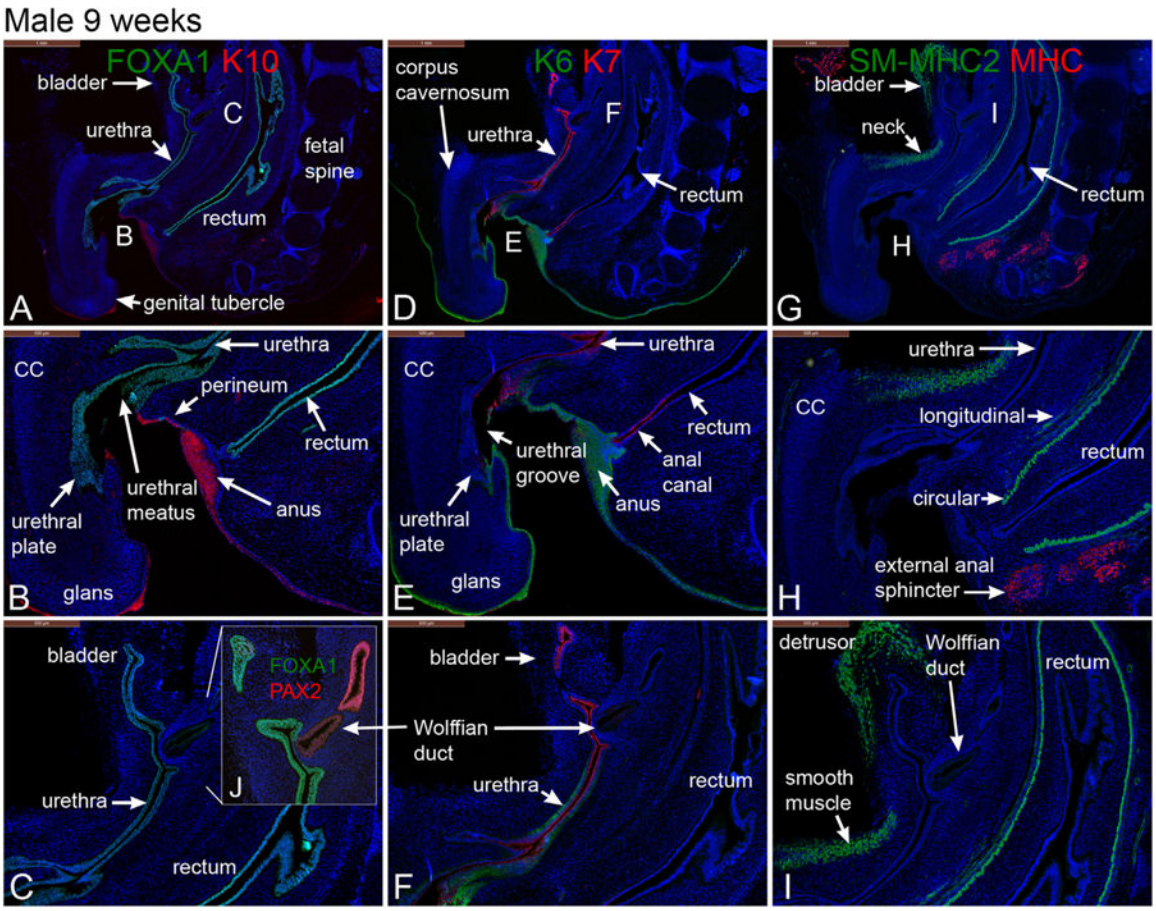

Fig. 2.

Mid-sagittal sections of a 9-week gestation male pelvis stained for FOXA1 and cytokeratin (K) 10 (A & B), FOXA1 and Pax2 (C), keratins 6 & 7 (K6, K7) (D, E & F), smooth muscle myosin heavy chain 2 (SM-MHC2) and myosin heavy chain (MHC) (G, H & I). Note the angulation of the genital tubercle to the body wall.

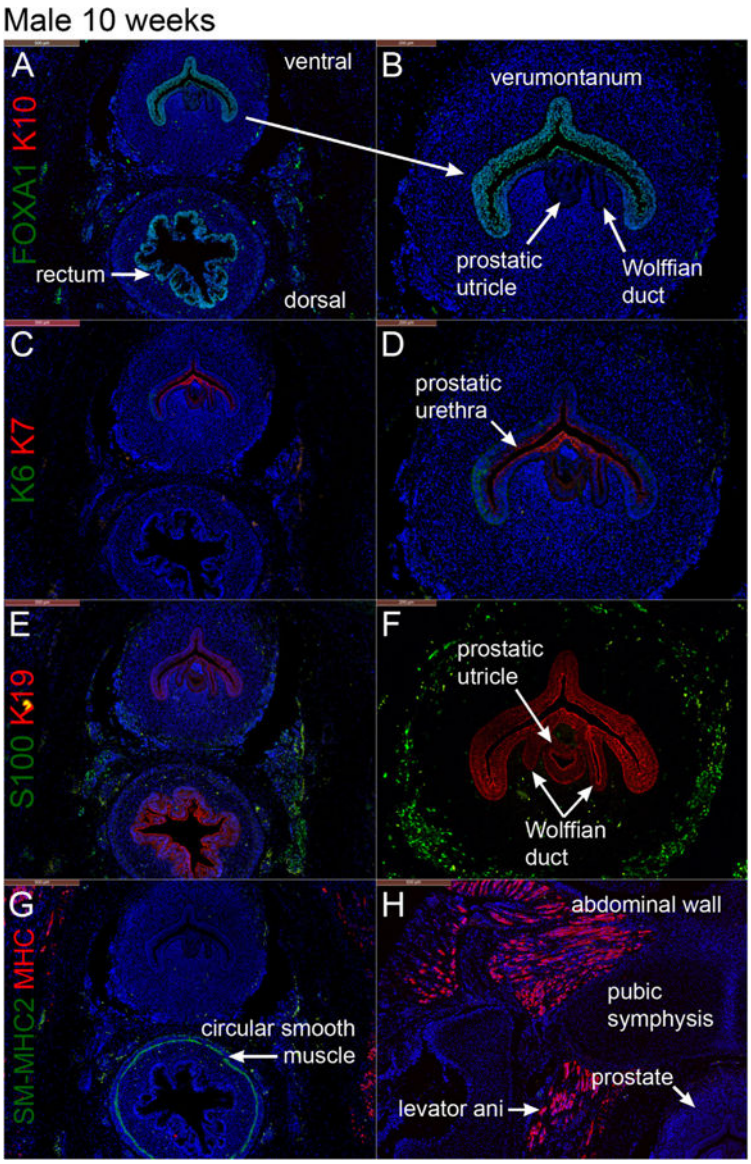

Fig. 3.

Transverse sections through the verumontanum (male specimen) and rectum at 10 weeks of gestation. Prostatic buds have not yet formed. A & B stained for FOXA1 and cytokeratin 10 (K10), C & D stained for keratins 6 and 7 (K6 and K7), E & F stained for S100 (nerve stain) and keratin 19 (K19), and G and H stained for smooth muscle myosin heavy chain 2 (SM-MHC2) and myosin heavy chain (MHC).

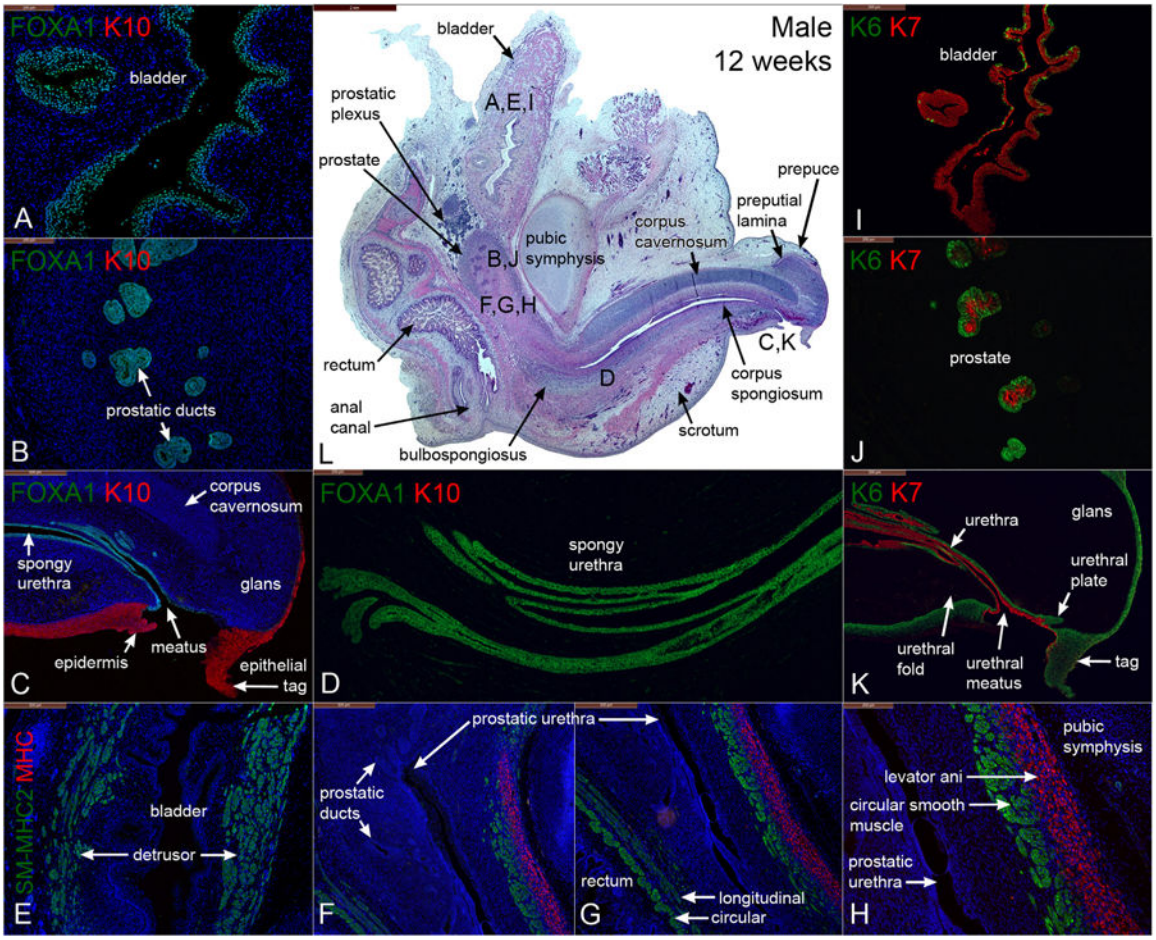

Fig. 4.

Mid-sagittal sections of a male pelvis at 12 weeks of gestation. (A-D) are stained for FOXA1 and KRT10 (K10), (E-H) are stained for smooth muscle myosin heavy chain 2 (SM-MHC2) and myosin heavy chain (MHC), (I-K) are stained for keratin 6 and 7 (K6 & K7). (L) is stained with H&E which is a low power image showing the locations of sections (A-H). Note the penis is now oriented ~90 degrees pointing outward from the abdominal wall.

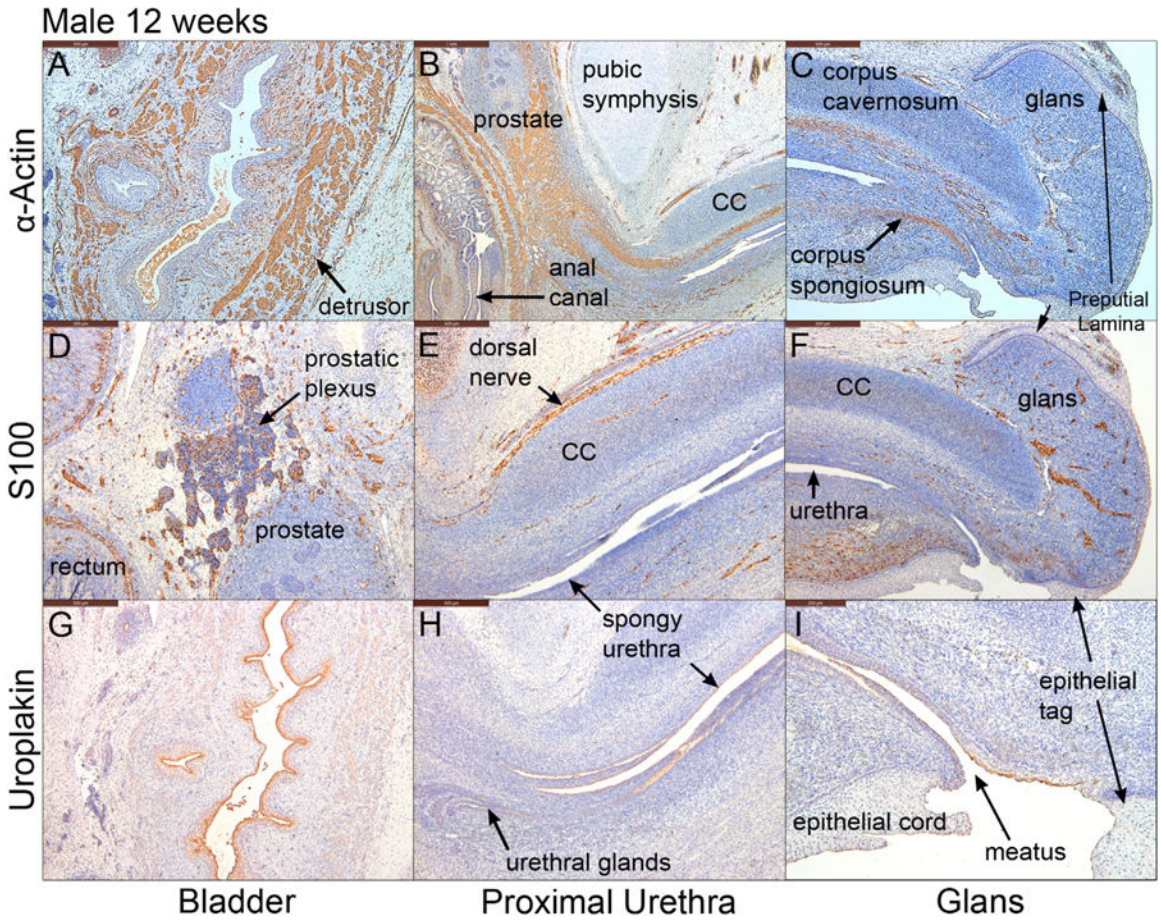

Fig. 5.

Mid-sagittal sections of a male pelvis at 12 weeks of gestation. A-C stained for α-actin, D-F stained for S100 and G-I stained for uroplakin. Note uroplakin stains superficial epithelial cells of the urothelium in the bladder, the urethra and the urethral meatus. CC=corpus cavernosum.

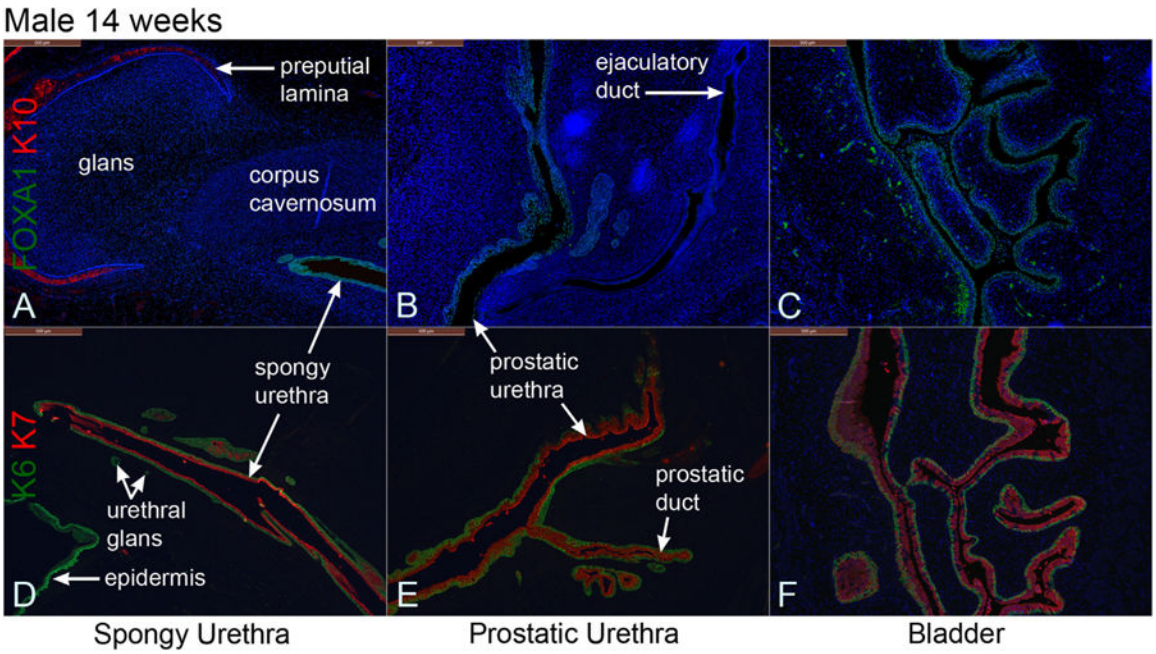

Fig. 6.

Mid-sagittal sections of a 14-week male pelvis. A–C stained for FOXA1 and cytokeratin 10 (K10). D–F stained for keratins 6 and 7 (K6 and K7). FOXA1 stains epithelia of the bladder, prostatic urethra and spongy urethra. Keratin 6 was expressed in basal epithelial layers, and keratin 7 was expressed in apical epithelial layers of these organs.

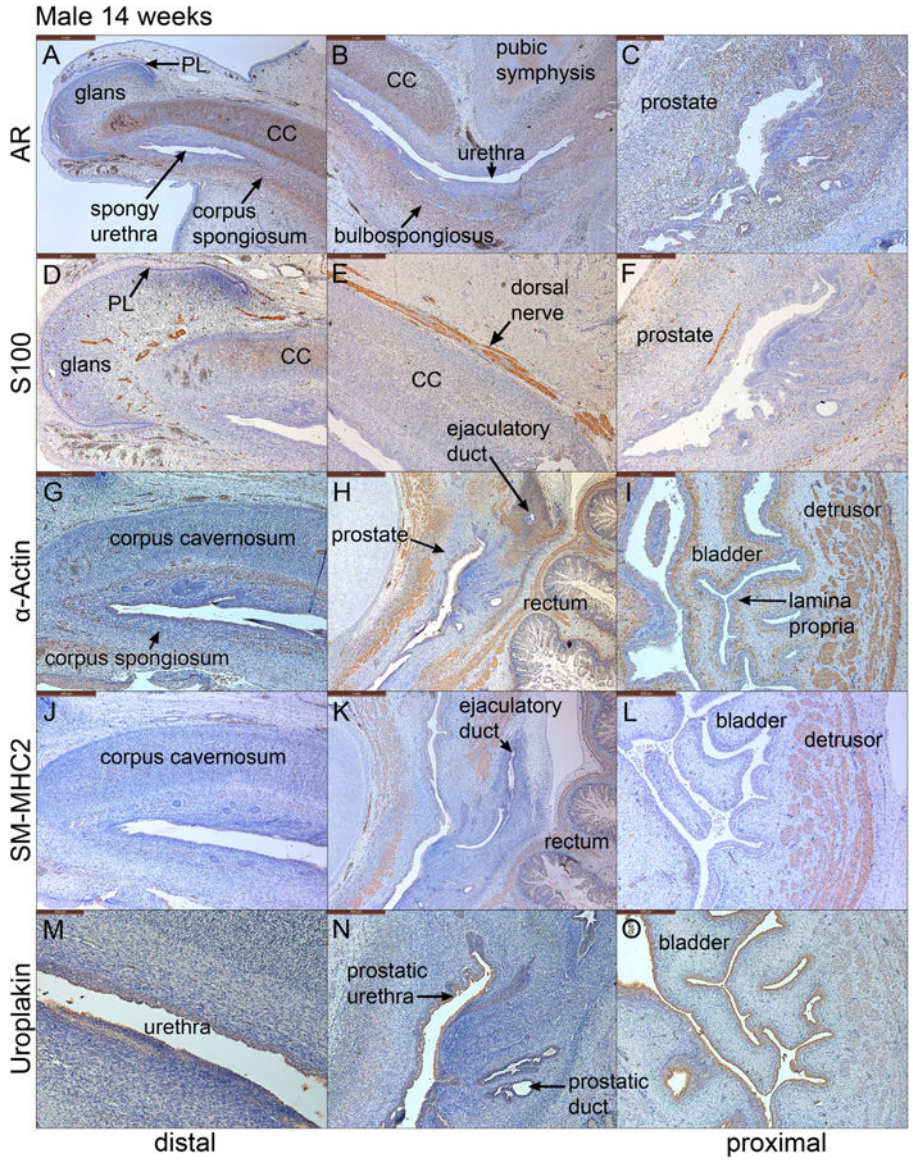

Fig. 7.

Mid-sagittal sections of a 14-week male pelvis. A-C stained for androgen receptor (AR), D–F stained for S100, G–I stained with α-actin, J–L stained for SM-MHC2 and M-O stained for uroplakin. Note the strong expression of AR in the corpus cavernosum (CC), corpus spongiosum, glans penis and prostate. S100-reactive nerves were detected in the prostate (F), the penile shaft (E) and the penile glans. α−Actin and SM-MHC2, markers of smooth muscle, were detected in the penis, the urethra and bladder (G–L). Uroplakin is seen in epithelia of the urethra and bladder (M-O). PL = preputial lamina.

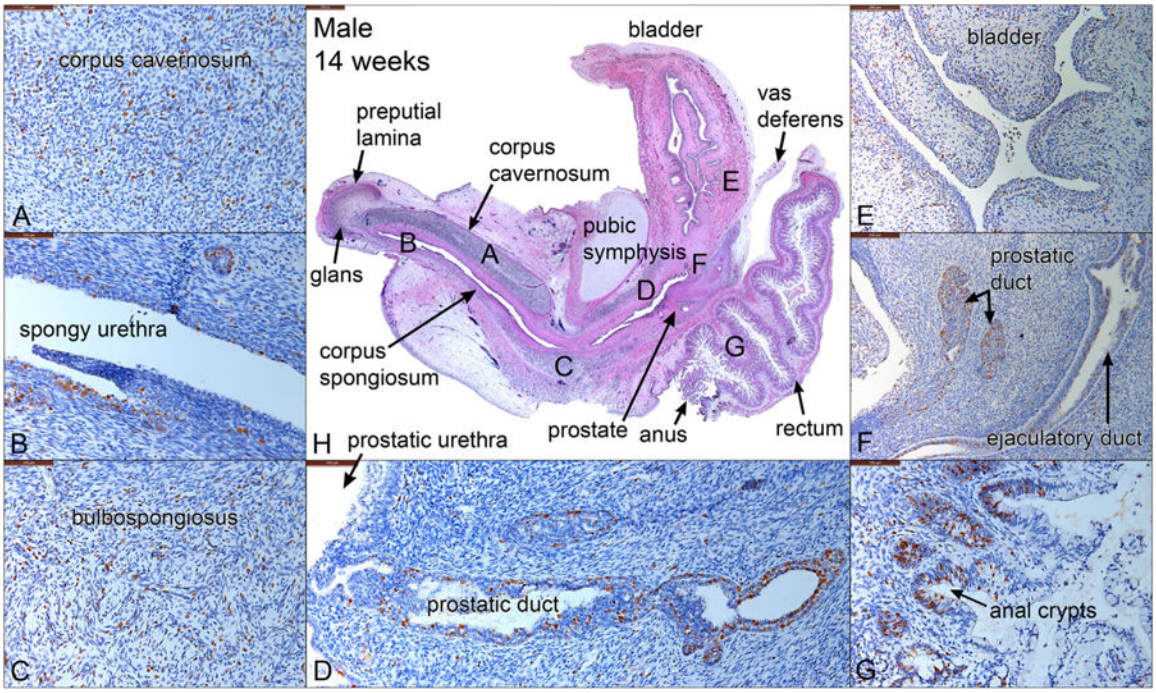

Fig. 8.

Mid-sagittal sections of a 14-week male pelvis. (A-G) stained with Ki67, a cellular proliferation marker. (H) stained with H&E, which is a low power view labeled with the location of the high-power images in A-G. Note areas of cellular proliferation in each panel.

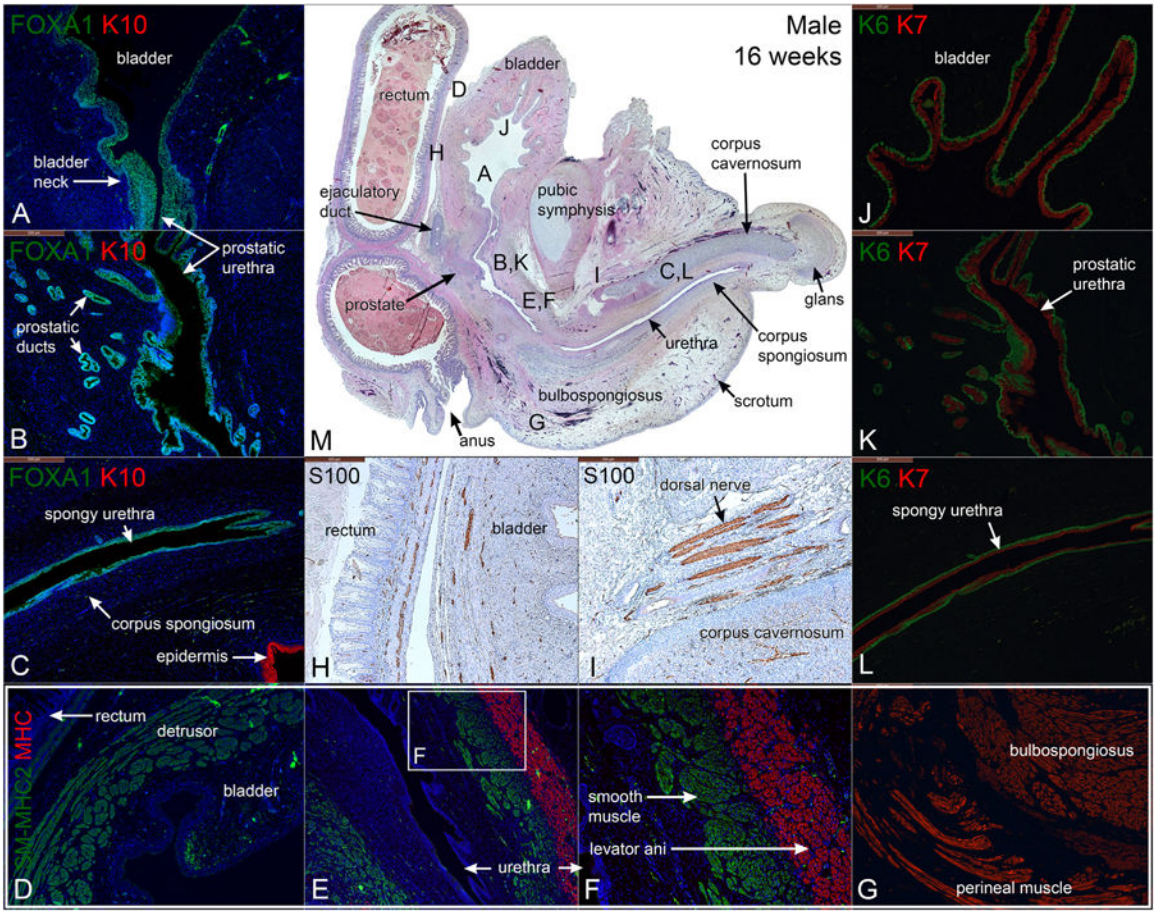

Fig. 9.

Mid-sagittal sections of a 16-week male pelvis. A–C stained for FOXA1 and keratin 10 (K10), D–G stained for smooth muscle myosin heavy chain 2 (SM-MHC2) and myosin heavy chain (MHC), J–L stained for keratin 6 and 7 (K6 & K7), H & I stained for S100 and M stained with H & E, which is a low power image showing the location of A–I. Note the mirror expression of FOXA1 and KRT7 in the bladder, bladder neck and the urethra.

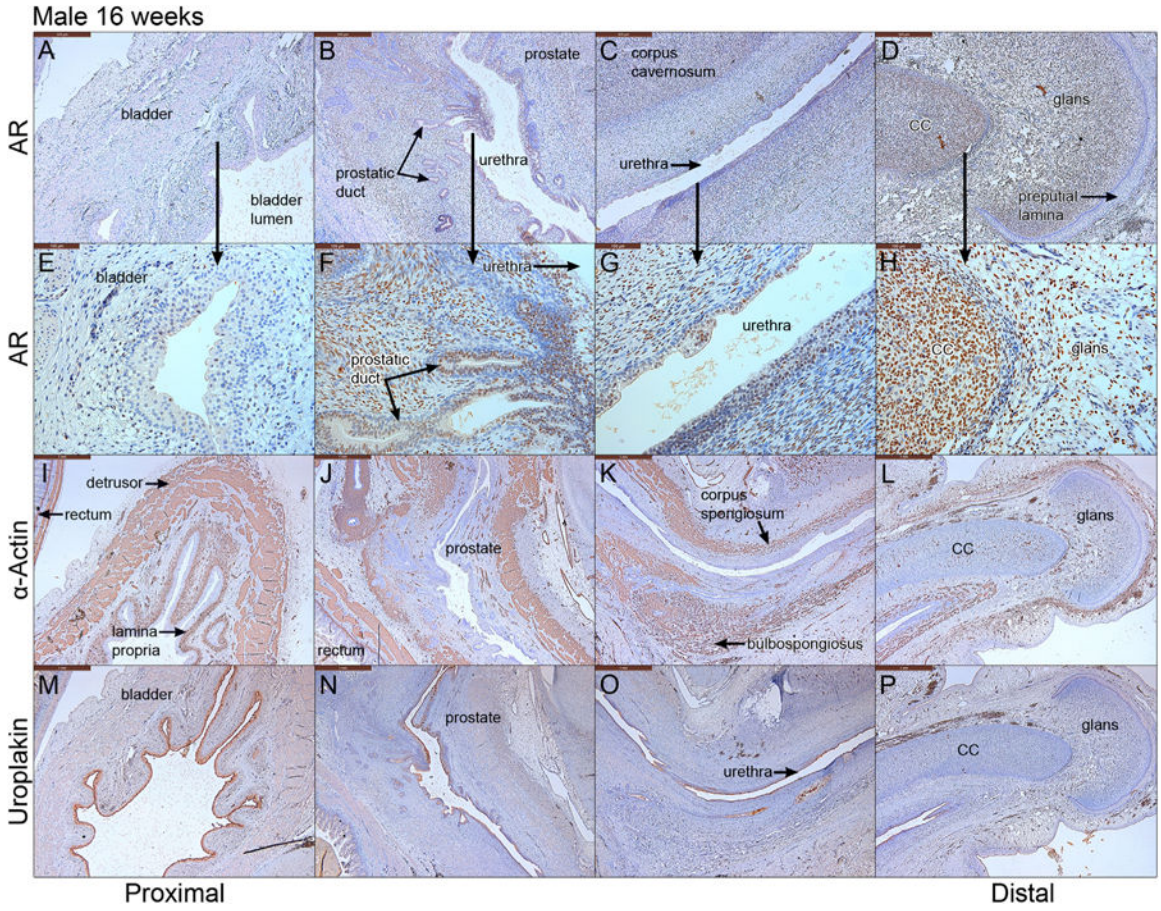

Fig. 10.

Mid-sagittal sections of a 16-week male pelvis from proximal to distal. A–D stained for androgen receptor (AR), E–H high power of A–D, I–L stained for α-actin, M–P stained for uroplakin. cc= corpus cavernosum.

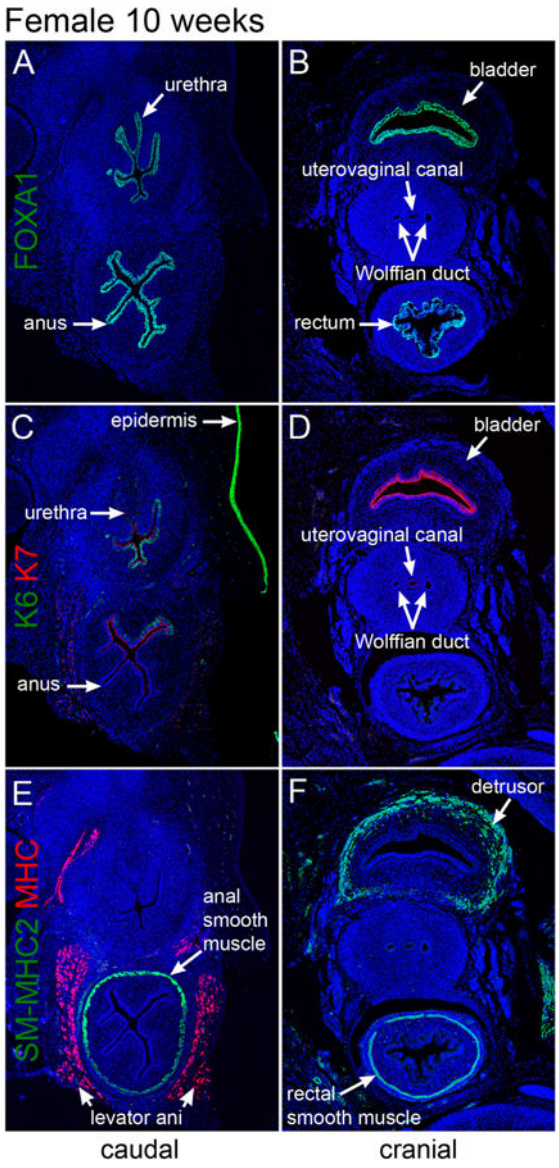

Fig. 11.

Transverse sections through the bladder, urethra, rectum and anus of a 10-week female specimen. A & B stained for FoxA1, C & D stained for keratins 6 and 7 (K6 and K7), E & F stained for smooth muscle myosin heavy chain 2 (SM-MHC2) and myosin heavy chain (MHC).

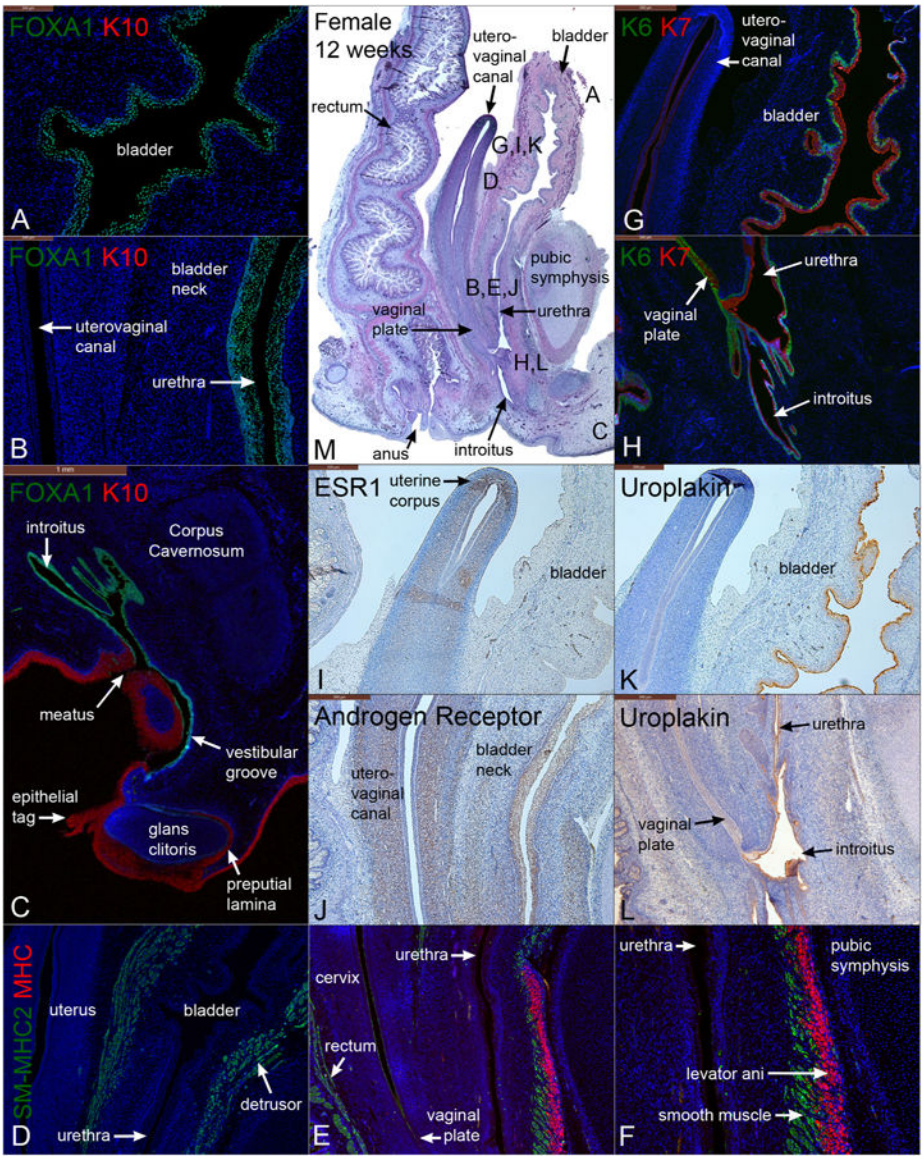

Fig. 12.

Mid-sagittal sections of a female pelvis at 12 weeks of gestation. (A–C) are stained for FOXA1 and keratin 10 (K10). (D–F) are stained for smooth muscle myosin heavy chain 2 (SM-MHC2) and myosin heavy chain (MHC). (G–H) are stained for keratins 6 and 7 (K6 & K7). (I) is stained for estrogen receptor 1 (ESR1). (J) is stained for androgen receptor (AR). (K & L) are stained for uroplakin. (M) is stained with H&E which is a low power showing the location of A-L.

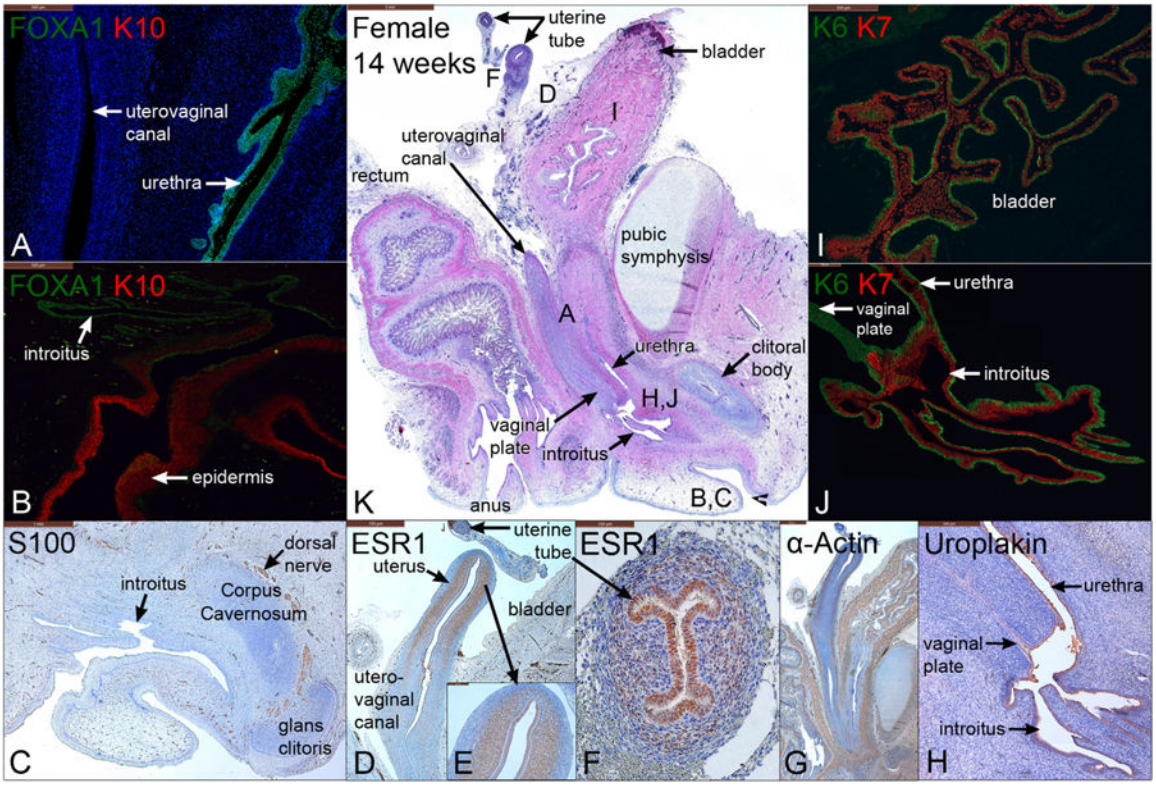

Fig. 13.

Mid-sagittal sections of a female pelvis at 14 weeks of gestation. A–B are stained for FOXA1 and keratin 10 (K10), C is stained for S100 to reveal nerves, D–F are stained for estrogen receptor 1 (ESR1), G is stained for α-actin, H is stained for uroplakin, I–J are stained for keratins 6 and 7 (K6 and 7), and K is stained with H & E which is a low power showing the location of A–J.

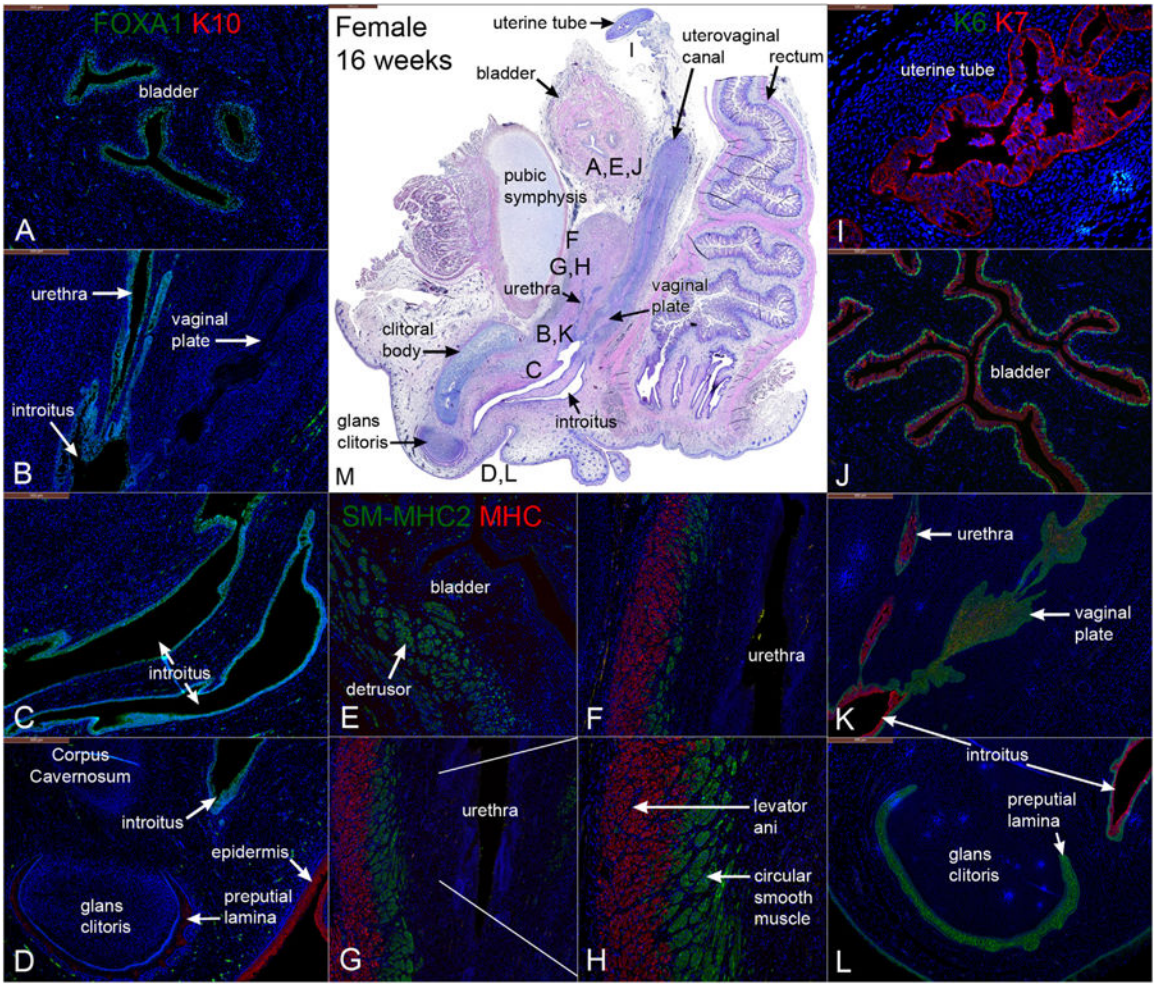

Fig. 14.

Mid-sagittal sections of a 16-week gestation female pelvis. (A–D) are stained for FOXA1 and keratin10 (K10). (E–H) are stained for smooth muscle myosin heavy chain 2 (SM-MHC2) and myosin heavy chain (MHC) (A&B). (I–L) are stained for keratins 6 and 7 (K6 & K7). (M) is stained with H & E which is a low power showing the location of A–L.

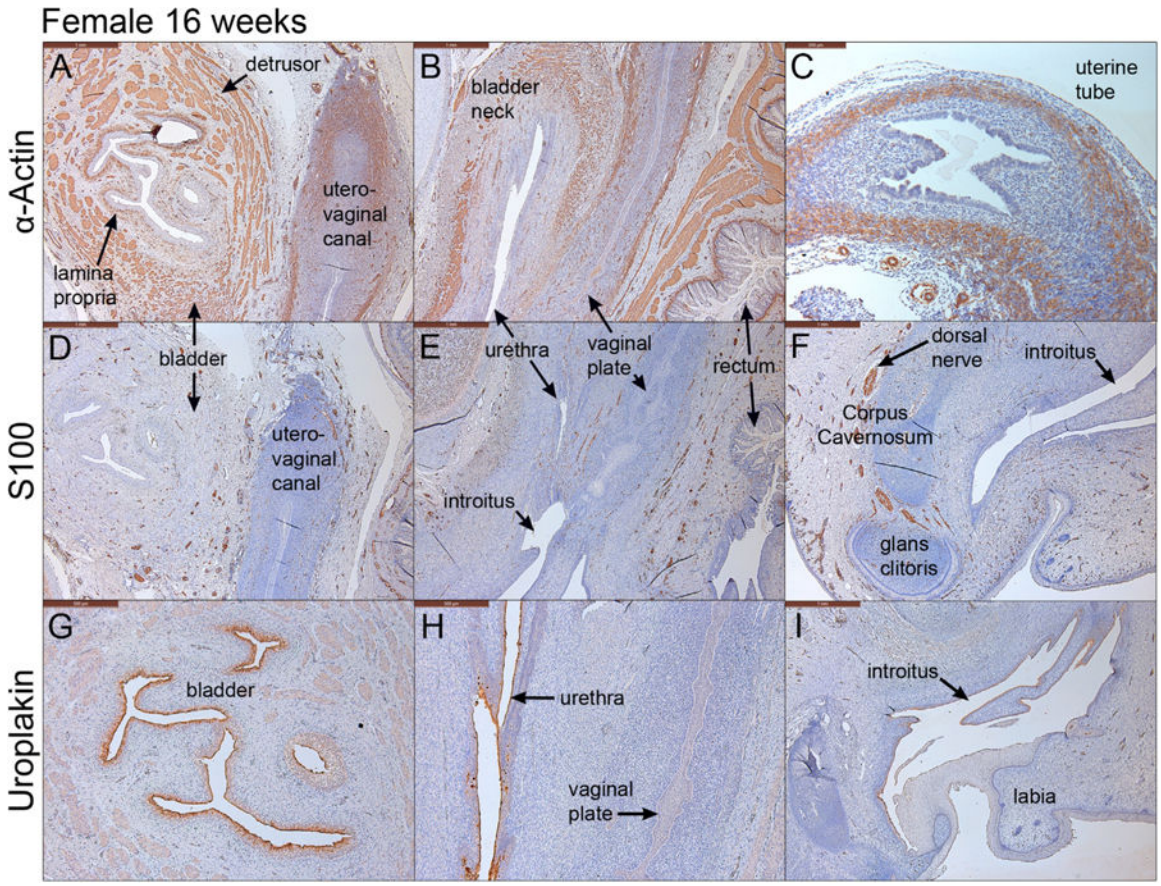

Fig. 15.

Mid-sagittal sections of a female pelvis at 16 weeks of gestation. (A–C) are stained for α-actin. (D–F) are stained for the non specific neuronal marker, S100. (G–I) are stained for uroplakin. α-actin stains the smooth muscle in the bladder, uterovaginal canal and uterine tube (A–C). Uroplakin stains the urothelium in the bladder, urethra and at the introitus/urethral meatus (G–I).

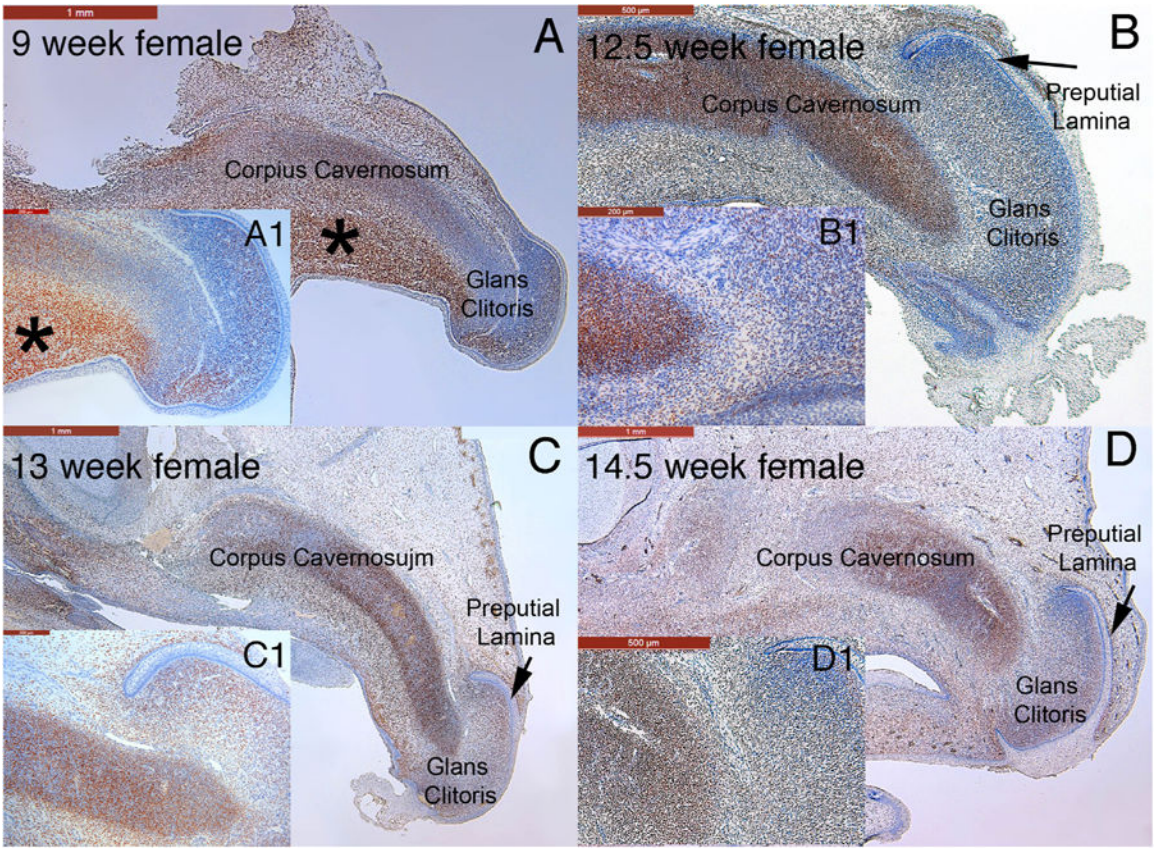

Fig. 16.

Mid-sagittal sections stained for the androgen receptor in the developing human female genital tubercle at 9 weeks of gestation (A) and clitoris at 12.5, 13 and 14.5 weeks of gestation (B-D, respectively). Note the strong localization of the androgen receptor to the corpus cavernosum and glans clitoris at all fetal ages. In the 9-week specimen note especially strong staining of the androgen receptor in the mesenchyme below the corpus cavernosum (* in A). A1-D1 are high power images of each time point.

Table 1

Antibodies used in this study.

Antibody	Concentrations	Source
Androgen Receptor	1/100	Genetex, USA
Estrogen Receptor α	1/100	Abcam, USA
Cytokeratin 6	1/200	Acris, Germany
Cytokeratin 7 (LDS-68 clone)	1/10	Sigma, Israel
Cytokeratin 10	1/50	Dako, USA
Cytokeratin 19 (K 4.64 clone)	1/5	Sigma St. Louis, USA
PAX2	1/25	Abcam, USA
FOXA1	1/100	Atlas Antibodies, Sweden
Uroplakin	1/500	Gift Henry Sun, NYU
Myosin Heavy Chain (MF20)	1/100	R & D Systems, USA
Smooth Muscle α Actin	1/500	Sigma St. Louis, USA
Smooth Muscle Myosin Heavy Chain 2	1/100	Abcam, USA
KI67	1/200	Leica Biosystems, USA
S100	1/1000	Abcam, USA